NASA TECHNICAL MEMORANDUM

NASA TM X-3298

NASA TM X-3298

THRUST PERFORMANCE OF ISOLATED 36-CHUTE SUPPRESSOR PLUG NOZZLES WITH AND WITHOUT EJECTORS AT MACH NUMBERS FROM 0 TO 0.45

Douglas E. Harrington, James J. Schloemer, and Stanley A. Skebe

Lewis Research Center
Cleveland, Ohio 44135

NATIONAL AERONAUTICS AND SPACE ADMINISTRATION • WASHINGTON, D. C. • OCTOBER 1975

1. Report No. NASA TM X-3298	2. Government Accession No.	3. Recipient's Catalog No.
4. Title and Subtitle THRUST PERFORMANCE OF ISOLATED 36-CHUTE SUPPRESSOR PLUG NOZZLES WITH AND WITHOUT EJECTORS AT MACH NUMBERS FROM 0 TO 0.45		5. Report Date October 1975
		6. Performing Organization Code
7. Author(s) Douglas E. Harrington, Lewis Research Center; James J. Schloemer, General Electric Company, Cincinnati, Ohio; and Stanley A. Skebe, Lewis Research Center		8. Performing Organization Report No. E-8334
9. Performing Organization Name and Address Lewis Research Center National Aeronautics and Space Administration Cleveland, Ohio 44135		10. Work Unit No. 505-11
		11. Contract or Grant No.
12. Sponsoring Agency Name and Address National Aeronautics and Space Administration Washington, D. C. 20546		13. Type of Report and Period Covered Technical Memorandum
		14. Sponsoring Agency Code
15. Supplementary Notes		

16. Abstract

Plug nozzles with chute-type noise suppressors were tested with and without ejector shrouds at free-stream Mach numbers from 0 to 0.45 and over a range of nozzle pressure ratios from 2 to 4. A 36-chute suppressor nozzle with an ejector had an efficiency of 94.6 percent at an assumed takeoff pressure ratio of 3.0 and a Mach number of 0.36. This represents only a 3.4 percent performance penalty when compared with the 98 percent efficiency obtained with a previously tested unsuppressed plug nozzle.

17. Key Words (Suggested by Author(s))	18. Distribution Statement
Exhaust nozzles; Nozzles; Plug nozzles; Noise suppression; Jet noise; Suppressor nozzles	Unclassified - unlimited STAR Category 07 (rev.)

19. Security Classif. (of this report)	20. Security Classif. (of this page)	21. No. of Pages	22. Price*
Unclassified	Unclassified	45	$3.75

* For sale by the National Technical Information Service, Springfield, Virginia 22161

THRUST PERFORMANCE OF ISOLATED 36-CHUTE SUPPRESSOR PLUG NOZZLES WITH AND WITHOUT EJECTORS AT MACH NUMBERS FROM 0 TO 0.45

by Douglas E. Harrington, James J. Schloemer*, and Stanley A. Skebe

Lewis Research Center

SUMMARY

Several 36-chute suppressor plug nozzles were tested with and without ejectors in the Lewis 8- by 6-Foot Supersonic Wind Tunnel to determine thrust performance at takeoff conditions. These nozzles were designed primarily for application to advanced supersonic-cruise aircraft in which a dry turbojet or mixed-flow turbofan engine would be used. Data were obtained at free-stream Mach numbers from 0 to 0.45 and nozzle pressure ratios of 2.0 to 4.0. Dry air at approximately tunnel total temperature (32° C (90° F)) was supplied to the nozzles in this test.

A deep-chute suppressor nozzle without an ejector exhibited a nozzle efficiency of 94.1 percent at an assumed takeoff pressure ratio of 3.0 and a Mach number of 0.36. The same nozzle with a setback ejector had an efficiency of 94.6 percent. These efficiencies represent decreases in nozzle performance of 3.9 and 3.4 percent, respectively, when compared with an unsuppressed plug nozzle. A shallow-chute suppressor nozzle without an ejector shroud had a nozzle efficiency of 91.2 percent at the assumed takeoff condition. Addition of the setback ejector to this nozzle reduced efficiency to 90 percent. These efficiencies represent decreases in nozzle performance of 6.8 and 8 percent, respectively, when compared with an unsuppressed plug nozzle. The thrust loss of these suppressor nozzles relative to an unsuppressed plug nozzle was due primarily to chute-base pressure drag. For example, at the assumed takeoff condition the deep-chute suppressor without an ejector had a chute-base pressure drag equal to 4 percent of ideal thrust. This represents 100 percent of the loss relative to the unsuppressed plug nozzle. At the takeoff nozzle pressure ratio of 3.0, nozzle efficiency for all suppressor nozzles was sensitive to external flow. For example, at Mach 0.36 the deep-chute suppressor nozzle without an ejector experienced a thrust loss of approximately 3 percent when compared with static performance.

---

*General Electric Company, Cincinnati, Ohio.

INTRODUCTION

Nozzle concepts appropriate for advanced supersonic-cruise aircraft must operate efficiently over a wide range of flight conditions and engine power settings. The low-angle conical plug is a nozzle concept that offers the potential of good aerodynamic performance with a minimum of mechanical complexity. As a consequence, a number of tests have been conducted (refs. 1 to 11) to optimize the thrust performance, to investigate installation effects, and to determine the heat-transfer characteristics for this type of plug nozzle.

In recent years, increasing emphasis has been placed on the reduction of aircraft noise. During takeoff and climb-out, when aircraft engines are at a high power setting, the dominant noise source is usually associated with the high-velocity jet emanating from the exhaust nozzle. Jet noise characteristics for several nozzle types, including a low-angle plug, were evaluated at takeoff pressure ratios in a static test stand (ref. 12). However, takeoff and climb-out speeds associated with advanced supersonic aircraft are relatively high (~Mach 0.35). Thus, the effect of forward velocity on jet noise must also be evaluated. Tests to evaluate flight velocity effects have been conducted and are reported in references 13 to 20.

A number of techniques to suppress jet noise are currently under investigation. Several concepts of interest, particularly for plug nozzles, are the multispoke and multichute suppressors. During takeoff and climb-out, these multielement suppressors are deployed for jet noise suppression. After climb-out from the airport the chutes are retracted into the plug or outer shroud for cruise. In order to evaluate a suppressor concept like the multichute, it is necessary to study a trade-off between high noise suppression and good thrust performance (refs. 21 to 24). A previous test (ref. 24) investigated the thrust performance of two types of 40-spoke suppressor. However, these nozzles were designed to optimize noise suppression, and they incurred relatively low thrust performance (~83 to 84 percent at assumed takeoff conditions). The suppressor nozzles that were tested in the current investigation were designed to have high thrust performance by using chutes which would improve base flow ventilation.

This report presents the thrust performance of various 36-chute suppressor plug nozzles tested in the Lewis 8- by 6-Foot Supersonic Wind Tunnel. These nozzles were tested with and without ejector shrouds and were designed primarily for application to advanced supersonic-cruise aircraft in which a dry turbojet or mixed-flow turbofan engine would be used. A Supersonic Tunnel Association (STA) nozzle was also tested to provide a baseline level of thrust performance. Data were obtained at free-stream Mach numbers from 0 to 0.45 and nozzle pressure ratios of 2.0 to 4.0. Dry air at approximately tunnel total temperature (32° C (90° F)) was supplied to the nozzles in this test. Model angle of attack was maintained at 0°. The range of Reynolds number was from

8.01×10^6 to 9.38×10^6 per meter (2.44×10^6 to 2.86×10^6 per ft) at Mach numbers from 0.36 to 0.45, respectively.

APPARATUS AND PROCEDURE

Installation

The test nozzles were strut mounted in the test section of the wind tunnel, as shown in figures 1 and 2. The support system consisted of a strut (0° sweep) having a thickness-to-chord ratio of 0.036 and a forebody with a maximum diameter of 21.59 centimeters (8.5 in.). Because the nozzles in this test were 20.32 centimeters (8.0 in.) in diameter, a transition section was necessary to adapt the 20.32-centimeter (8.0-in.) diameter nozzles to the support forebody diameter of 21.59 centimeters (8.5 in.). The transition section was 2.9 nozzle diameters in length. A cylindrical section approximately 3.75 nozzle diameters long was provided downstream of the transition. The cone-cylinder pressure data of reference 25 indicate that this section should have been of sufficient length to reestablish ambient flow conditions. The thrust-minus-drag of the exhaust nozzles was determined from the force- and flow-measuring section located just downstream of the transition section (fig. 2).

The internal geometry of the model showing the details of the force- and flow-measuring section is shown in figure 3. Nozzle weight flow was determined by using a choked long-radius ASME nozzle with a diverging section. Because the metering nozzle was choked, it was necessary to measure only total pressure and temperature. Total pressure P_1 upstream of the flowmetering nozzle was measured by a four-tube, area-weighted rake. Total temperature T_1 was measured by two shielded thermocouples. In order to determine the actual weight flow of the test nozzle, it was necessary to calculate a meter discharge coefficient. In addition, real gas effects were accounted for in the determination of weight flow (ref. 26).

The metric part of the model was cantilevered directly from the diverging section of the flowmetering nozzle (fig. 3). Two strain-gage links were used to measure the force between the metric and grounded parts of the model. A flexible seal at the throat of the flowmetering nozzle was used to separate the metric and grounded sections. The actual thrust-minus-drag of a test nozzle was then determined from the momentum entering the throat of the flowmetering nozzle, a balance force obtained from the two strain-gage links, and various pressure-area terms. When testing with external flow, the thrust-minus-drag of the test nozzle as so calculated was modified to exclude the friction drag on the surface from the metric break to the beginning of the test nozzle (approximately 1.5 nozzle diameters). This drag was estimated by the method of K. D. Smith (Rep. ARC-CP-824, Air Research Council, Gr. Britain).

The nozzle airflow passed through a series of choke plates and screens to provide uniform flow at station 7. The nozzle total pressure at this station P_7 was determined by using two four-tube area-weighted rakes. Nozzle total temperature T_7 was calculated by subtracting the temperature drop due to Joule-Thomson throttling of a real gas between stations 1 and 7. This temperature drop was calculated by using a curve fit of tabulated properties of air from reference 27. The model pressures, except the high total pressure P_1, were determined with a scanner valve system. The pressure P_1 was determined by four individual pressure transducers.

During a test run the procedure was to set a free-stream Mach number and then go through a variation in nozzle pressure ratio. Since tunnel static pressure was constant for a given free-stream Mach number, variations in nozzle pressure ratio were obtained by changing nozzle total pressure P_7.

Nozzle Geometry

The geometric details of the various nozzles tested are shown in figure 4. Pertinent area ratios are listed in table I. The STA nozzle is shown in figure 4(a). This nozzle is basically a modified ASME nozzle with a circular-arc boattail. The STA nozzle was tested to provide a reference level of performance for this particular installation in the wind tunnel.

The suppressor nozzles (figs. 4(b) and (c)) were tested both with and without ejector shrouds. The suppressor nozzles evaluated in this test each had a 15° half-angle plug and 36 chutes. Each chute was slanted 15° forward from vertical and was normal to the plug surface (to increase thrust performance by directing the flow along the plug surface). Each chute was open and formed a "vee" (view A-A, fig. 4(b)). The "vee" is intended to improve ventilation in the chute-base region and to improve mixing of the nozzle jet with the external flow. The chutes were run in both deep and shallow modes, the latter formed by fitting an insert into the deep chute. The geometric area ratio $(AR)_{geo}$ of these suppressor nozzles was approximately 2.29. The geometric area ratio is defined as the ratio of the annular flow area with chutes retracted to the geometric flow area with chutes deployed.

The suppressor nozzles (both deep and shallow chute) were also tested with two types of ejector, setback and large inlet, as shown in figure 4(c). These ejectors were designed to reduce jet noise by promoting the mixing of external air with the nozzle jet. They can also be used as an acoustically treated surface for further noise reduction. The setback ejector was inclined 8.5° to the horizontal in order to maintain a convergent flow area between the ejector shroud and the plug. The large-inlet ejector was inclined 6.8° to the horizontal for the same reason. Both ejectors were attached to the nozzle by nine struts.

Instrumentation

Instrumentation for the test nozzles is presented in figures 5 and 6. Static-pressure orifices are denoted by solid symbols but do not necessarily represent the true circumferential locations of the orifices. The accompanying tables give the correct circumferential location of each orifice and its axial location. For the STA nozzle, the axial reference point ($X_\beta = 0$) is the tangent point of the nozzle boattail with the cylindrical section of the model. For the suppressor nozzles the axial reference point ($X = 0$) was chosen to be the location of the nozzle geometric throat at the plug surface. Orifice locations for measuring chute-base pressure drag are tabulated as a function of circumferential location and a dimensionless radius parameter R.

The characteristics of the boundary layer approaching the test nozzles were determined by separately testing a cylindrical shroud with a total pressure rake. The details of the shroud and rake are shown in figure 7. The axial location of the rake corresponded to a location that was just upstream of where the suppressor nozzles were located during testing. This location was also approximately 18 model diameters from the nose of the model. The rake was located 45^o from the top centerline of the model ($\varphi = 45^o$) and consisted of 11 tubes.

RESULTS AND DISCUSSION

Nozzle efficiencies of the Supersonic Tunnel Association (STA) nozzle are presented in figure 8. Over the range of Mach numbers and nozzle pressure ratios tested, a comparison was made among data measured during this test, unpublished data, and data reported in reference 24. Data agreement was in general within 1/2 percent over the range of Mach numbers and nozzle pressure ratios.

Nozzle efficiencies of an unsuppressed plug nozzle (ref. 24) and the 36-deep-chute nozzle, with and without the setback and large-inlet ejectors, are presented as a function of nozzle pressure ratio in figure 9. For static conditions the deep-chute nozzle with the setback ejector had the highest nozzle efficiency at pressure ratios less than 3.75, with a peak efficiency of 1.004 at a nozzle pressure ratio of 3.25. This very high efficiency was due, no doubt, to the suction force on the ejector shroud at static conditions. The deep-chute nozzle without an ejector had a nozzle efficiency of 94.1 percent at an assumed takeoff pressure ratio of 3.0 and a Mach number of 0.36 (fig. 9(b)). The same nozzle with the setback ejector and with the large-inlet ejector had nozzle efficiencies of 94.6 and 92.7 percent, respectively, at the assumed takeoff condition. The unsuppressed plug nozzle at a pressure ratio of 3.0 and a Mach number of 0.36 had a nozzle efficiency of approximately 98 percent. The decrements in nozzle efficiency for the deep-chute suppressor nozzle without an ejector and with the setback and large-inlet ejectors were 3.9, 3.4, and 5.3 percent, respectively, when compared with the unsuppressed plug nozzle.

Nozzle efficiencies of the 36-shallow-chute nozzle, with and without the setback and large-inlet ejectors, are presented with the efficiencies of the unsuppressed plug nozzle (ref. 24) as a function of nozzle pressure ratio in figure 10. These four configurations were tested over the Mach number range of 0 to 0.45. For static conditions the shallow-chute nozzle with the setback ejector had the highest nozzle efficiency of the shallow-chute suppressor nozzles at pressure ratios greater than 2.5. The shallow-chute suppressor nozzle without an ejector shroud had a nozzle efficiency of 91.2 percent at a pressure ratio of 3.0 and a Mach number of 0.36 (fig. 10(b)). Addition of the setback ejector and the large-inlet ejector under these same conditions reduced these efficiencies to 90.0 and 88.9 percent, respectively. The decrements in nozzle efficiency for the shallow-chute suppressor nozzle without an ejector and with the setback and large-inlet ejectors were 6.8, 8.0, and 9.1 percent, respectively, when compared with the unsuppressed plug nozzle.

The chute-base pressure drag for the deep-chute suppressor nozzle with and without the ejector shrouds is presented in figure 11 as a fraction of nozzle ideal thrust. At all test Mach numbers the ratio of chute-base pressure drag to nozzle ideal thrust for the three deep-chute configurations decreased with increasing nozzle pressure ratio. This loss represents a significant part of the nozzle efficiency decrement between the unsuppressed plug nozzle and the deep-chute suppressor nozzles at Mach numbers from 0.36 to 0.45. For example, at an assumed takeoff Mach number of 0.36 and pressure ratio of 3.0, the chute-base pressure drag of the deep-chute suppressor nozzle without an ejector was 4.0 percent of nozzle ideal thrust (fig. 11(a)). This represents 100 percent of the loss relative to the unsuppressed plug nozzle (fig. 9(b)). The chute-base pressure drag of the suppressor nozzles with ejectors generally exceeded the chute-base pressure drag of the suppressor nozzles without ejectors. For example, the addition of the setback ejector to the deep-chute suppressor nozzle at the assumed takeoff condition increased the chute-base pressure drag from 4 percent to 5.4 percent of ideal thrust. This 5.4 percent loss (fig. 11(b)) exceeded the 3.4 percent overall thrust decrement when compared with an unsuppressed plug nozzle (fig. 9(b)).

It can be inferred from the preceding discussion and plug-pressure distributions (fig. 20) that some of the loss due to chute-base drag was offset by thrust augmentation on the ejector. This trend was not apparent with the addition of the large-inlet ejector to the deep-chute suppressor nozzle. The 5.0 percent thrust loss (fig. 11(c)) resulting from chute-base pressure drag was less than the 5.3 percent overall efficiency decrement (fig. 9(b)) relative to an unsuppressed plug nozzle. Thus, for this particular configuration it appears that no thrust augmentation was obtained from the large-inlet ejector.

Chute-base pressure drag for the shallow-chute suppressor nozzle with and without the ejector shrouds is presented in figure 12 as a fraction of nozzle ideal thrust. As with the deep-chute nozzles the chute-base pressure drag of the shallow-chute nozzle with either ejector exceeded the chute-base pressure drag of the shallow-chute nozzle without an ejector. For example, at the assumed takeoff conditions the chute-base pressure drag of the shallow-chute suppressor nozzle without an ejector was 7.5 percent of ideal thrust. Addition of the setback and large-inlet ejectors increased the chute-base pressure drag to 11.1 and 9.1 percent, respectively.

Chute-base pressure drag is also presented in coefficient form in figures 13 and 14 for all suppressor nozzles tested. In general, chute-base pressure drag coefficients peaked at nozzle pressure ratios from about 2.5 to 3.5.

In figure 15 the effect of external flow on nozzle efficiencies for the suppressor nozzles is presented at an assumed takeoff nozzle pressure ratio of 3.0. The efficiency of all the suppressor nozzles was sensitive to the addition of external flow. For example, at Mach 0.36 the deep-chute suppressor nozzle without an ejector experienced a thrust loss of approximately 3 percent when compared with its static performance. A further thrust loss of about 1.0 percent was experienced when the Mach number was increased to 0.45. At Mach 0.36 the deep-chute/setback-ejector nozzle experienced a thrust loss of approximately 5.5 percent when compared with its static performance. This configuration also experienced a further thrust loss of about 1.3 percent when the Mach number was increased to 0.45.

The shallow-chute suppressor nozzles were even more sensitive to external flow (fig. 15(b)). At Mach 0.36 the shallow-chute suppressor nozzle without an ejector experienced a thrust loss of approximately 5 percent when compared with its static performance. At the same Mach number the shallow-chute/setback-ejector nozzle experienced a thrust loss of approximately 8 percent. A further thrust loss of about 1.5 percent resulted for both nozzles when the Mach number was increased to 0.45. At a pressure ratio of 3.0 and over the range of Mach numbers tested, the suppressor nozzles with the large-inlet ejector had lower efficiencies than the other nozzles and also exhibited the same trend with external flow as the other nozzles.

Nozzle discharge coefficients of the STA and suppressor nozzles are presented in figures 16 and 17 as a function of nozzle pressure ratio. In each case, standard deviation was calculated and then used to develop a 95-percent confidence band. The largest spread for the STA nozzle was 1.7 percent at a nozzle pressure ratio of 2.5. This scatter would only slightly affect nozzle performance because of the thrust-measuring system design. For example, at a nozzle pressure ratio of 3.0 a 1 percent error in weight flow would result in only about a 0.3 percent error in nozzle efficiency. For the suppressor nozzles the largest spread was approximately 1.2 percent. However, there was a tendency for the mean flow coefficient to increase with increasing nozzle pressure ratio. This phenomenon was due to chute deflection and the resultant increase in geometric nozzle throat area A_8. It in no way affected the validity of the suppressor nozzle efficiencies presented in this report.

Boundary-layer velocity profiles obtained with a cylindrical shroud are presented in figure 18. These profiles were measured approximately 18 nozzle diameters downstream of the nose. This axial station corresponds to a location just upstream of where the suppressor nozzles were tested. Also included in this figure are the normalized boundary-layer displacement thickness δ^*/d_m and momentum thickness δ^{**}/d_m.

Boattail pressure coefficients for the STA nozzle are shown in figure 19 for a Mach number of 0.36 and over a range of nozzle pressure ratios. Internal and external surface static pressure distributions are presented in figures 20 to 23. Distributions are shown at pertinent Mach numbers and nozzle pressure ratios.

SUMMARY OF RESULTS

Several 36-chute suppressor plug nozzles were tested with and without ejectors in the Lewis 8- by 6-Foot Supersonic Wind Tunnel to determine thrust performance at takeoff conditions. These nozzles were designed primarily for application to advanced supersonic-cruise aircraft in which a dry turbojet or mixed-flow turbofan engine would be used. Data were obtained at free-stream Mach numbers from 0 to 0.45 and nozzle pressure ratios of 2.0 to 4.0. Dry air at approximately tunnel total temperature (32° C (90° F)) was supplied to the nozzles in this test. The following results were obtained:

1. A deep-chute suppressor nozzle without an ejector shroud had a nozzle efficiency of 94.1 percent at an assumed takeoff pressure ratio of 3.0 and Mach number of 0.36. The same nozzle with the setback ejector had a nozzle efficiency of 94.6 percent at the assumed takeoff condition. These efficiencies represent decreases in nozzle performance of 3.9 and 3.4 percent, respectively, when compared with an unsuppressed plug nozzle.

2. A shallow-chute suppressor nozzle without an ejector shroud had a nozzle efficiency of 91.2 percent at the assumed takeoff condition. Addition of the setback ejector in this case reduced efficiency to 90 percent. These efficiencies represent decrements in nozzle performance of 6.8 and 8 percent, respectively, when compared with an unsuppressed plug nozzle.

3. For all suppressor nozzles tested the efficiency decrements relative to an unsuppressed plug nozzle were caused primarily by chute-base pressure drag. For example, at the assumed takeoff condition the deep-chute suppressor nozzle without an ejector had a chute-base pressure drag of 4 percent of ideal thrust. This represents 100 percent of the loss relative to the unsuppressed plug nozzle.

4. The chute-base pressure drag of the suppressor nozzles with ejectors generally exceeded the chute-base pressure drag of the suppressor nozzles without ejectors. For example, the addition of the setback ejector to the deep-chute suppressor nozzle at the assumed takeoff condition increased the chute-base pressure drag from 4 percent to 5.4 percent of ideal thrust. However, it can be inferred from the performance of the deep-chute/setback-ejector nozzle and from plug-pressure distributions that some of the loss due to chute-base drag was offset by thrust augmentation on the ejector. This thrust augmentation was not obtained with the large-inlet ejector configuration.

5. At the takeoff nozzle pressure ratio of 3.0, nozzle efficiency for all suppressor nozzles was sensitive to external flow. For example, at Mach 0.36 the deep-chute suppressor nozzle without an ejector experienced a thrust loss of approximately 3 percent when compared with its static performance.

Lewis Research Center,
National Aeronautics and Space Administration,
Cleveland, Ohio, June 16, 1975,
505-11.

APPENDIX - SYMBOLS

A	cross-sectional or projected area
$(AR)_{eff}$	effective area ratio; ratio of annular flow area with chutes retracted to effective flow area with chutes deployed
$(AR)_{geo}$	geometric area ratio; ratio of annular flow area with chutes retracted to geometric flow area with chutes deployed
C_{DCH}	chute pressure-drag coefficient, D_{ch}/q_0A_m
$C_{D\beta}$	boattail pressure-drag coefficient, D_{β}/q_0A_m
C_{D8}	nozzle discharge coefficient
C_p	pressure coefficient, $(p - p_0)/q_0$
D	pressure drag
D_t	total external drag (viscous and pressure)
d	diameter
F	nozzle gross thrust
$(F - D_t)/F_i$	nozzle efficiency (or gross thrust coefficient)
M	Mach number
m	nozzle mass flow
P	total pressure
p	static pressure
q	dynamic pressure
R	chute radius parameter, $(r - r_{pl})/(r_{sh} - r_{pl})$
r	radial distance from nozzle axis
r_{pl}	plug radius at nozzle geometric throat ($X = 0$)
r_{sh}	outer-shroud internal radius at nozzle geometric throat ($X = 0$)
V	velocity
X	axial distance downstream of geometric nozzle throat on plug surface
X_{β}	axial distance downstream of boattail tangency point (Supersonic Tunnel Association nozzle only)
y	radial distance measured from model surface
Z	axial distance measured upstream from apex of plug

δ^* boundary-layer displacement thickness

δ^{**} boundary-layer momentum thickness

φ circumferential angle measured from top of nacelle in clockwise direction (looking upstream)

Subscripts:

ch chute

i ideal (based on actual weight flow)

m maximum nozzle diameter

pl plug

sh shroud

t total

β boattail

0 free stream

1 flow-measuring station

7 nozzle inlet station

8 nozzle throat station

REFERENCES

1. Bresnahan, Donald L.; and Johns, Albert L.: Cold Flow Investigation of a Low Angle Turbojet Plug Nozzle with Fixed Throat and Translating Shroud at Mach Numbers from 0 to 2.0. NASA TM X-1619, 1968.
2. Wasko, Robert A.; and Harrington, Douglas E.: Performance of a Collapsible Plug Nozzle Having Either Two-Position Cylindrical or Variable Angle Floating Shrouds at Mach Numbers from 0 to 2.0. NASA TM X-1657, 1968.
3. Bresnahan, Donald L.: Experimental Investigation of a 10° Conical Turbojet Plug Nozzle with Translating Primary and Secondary Shrouds at Mach Numbers from 0 to 2.0. NASA TM X-1777, 1969.
4. Johns, Albert L.: Quiescent-Air Performance of a Truncated Turbojet Plug Nozzle with Shroud and Plug Base Flows from a Common Source. NASA TM X-1807, 1969.
5. Harrington, Douglas E.: Performance of a 10° Conical Plug Nozzle with Various Primary Flap and Nacelle Configurations at Mach Numbers from 0 to 1.97. NASA TM X-2086, 1971.
6. Harrington, Douglas E.: Performance of Convergent and Plug Nozzles at Mach Numbers from 0 to 1.97. NASA TM X-2112, 1970.
7. Huntley, Sidney C.; and Samanich, Nick E.: Performance of a 10° Conical Plug Nozzle Using a Turbojet Gas Generator. NASA TM X-52570, 1969.
8. Samanich, Nick E.; and Chamberlin, Roger: Flight Investigation of Installation Effects on a Plug Nozzle Installed on an Underwing Nacelle. NASA TM X-2295, 1971.
9. Jeracki, Robert J.; and Chenoweth, Francis C.: Coolant Flow Effects on the Performance of a Conical Plug Nozzle at Mach Numbers from 0 to 2.0. NASA TM X-2076, 1970.
10. Chenoweth, Francis C.; and Lieberman, Arthur: Experimental Investigation of Heat-Transfer Characteristics of a Film-Cooled Plug Nozzle with Translating Shroud. NASA TN D-6160, 1971.
11. Clark, John S.; and Lieberman, Arthur: Thermal Design Study of an Air-Cooled Plug-Nozzle System for a Supersonic-Cruise Aircraft. NASA TM X-2475, 1972.
12. Darchuk, George V.; and Balombin, Joseph R.: Noise Evaluation of Four Exhaust Nozzles for Afterburning Turbojet Engine. NASA TM X-2014, 1970.

13. Burley, Richard R.; and Karabinus, Raymond J.: Flyover and Static Tests to Investigate External Flow Effect on Jet Noise for Non-Suppressor and Suppressor Exhaust Nozzles. AIAA Paper 73-190, Jan. 1973.

14. Burley, Richard R.; Karabinus, Raymond J.; and Freedman, R. J.: Flight Investigation of Acoustic and Thrust Characteristics of Several Exhaust Nozzles Installed on Underwing Nacelles on an F-106 Airplane. NASA TM X-2854, 1973.

15. Chamberlin, Rober: Flyover and Static Tests to Study Flight Velocity Effects on Jet Noise of Suppressed and Unsuppressed Plug Nozzle Configurations. NASA TM X-2856, 1973.

16. Burley, Richard R.; and Head, V. L.: Flight Velocity Effects on Jet Noise of Several Variations of a 48-Tube Suppressor Installed on a Plug Nozzle. NASA TM X-2919, 1974.

17. Wilcox, F. A.: Comparison of Ground and Flight Test Results Using a Modified F-106B Aircraft. AIAA Paper 73-1305, Nov. 1973.

18. Burley, Richard R.: Flight Velocity Effects on the Jet Noise of Several Variations of a 104-Tube Suppressor Nozzle. NASA TM X-3049, 1974.

19. Simcox, C. D.; Armstrong, R. S.; and Atvars, J.: Recent Advances in Exhaust Systems for Jet Noise Suppression of High Speed Aircraft. AIAA Paper 75-333, Feb. 1975.

20. Burley, Richard R.; and Johns, Albert L.: Flight Velocity Effects on Jet Noise of Several Variations of a Twelve-Chute Suppressor Installed on a Plug Nozzle. NASA TM X-2918, 1974.

21. Bresnahan, Donald L.: Internal Performance of a 10° Conical Plug Nozzle with a Multispoke Primary and Translating External Shroud. NASA TM X-2573, 1972.

22. Johns, Albert L.: Internal Performance of a Wedge Nozzle for a Supersonic-Cruise Aircraft with a Multispoke Primary for Noise Suppression. NASA TM X-2689, 1973.

23. Brausch, J. F.: Flight Velocity Influence on Jet Noise of Conical Ejector, Annular Plug and Segmented Suppressor Nozzles. (General Electric Co.; NAS3-15773.) NASA CR-120961, 1972.

24. Harrington, Douglas E.; and Schloemer, James J.: Thrust Performance of Isolated Plug Nozzles with Two Types of 40-Spoke Noise Suppressor at Mach Numbers from 0 to 0.45. NASA TM X-2951, 1974.

25. Blaha, Bernard J.; and Bresnahan, Donald L.: Wind Tunnel Installation Effects on Isolated Afterbodies at Mach Numbers from 0.56 to 1.5. NASA TM X-52581, 1969.

26. Johnson, Robert C.: Real-Gas Effects in Critical-Flow-Through Nozzles and Tabulated Thermodynamic Properties. NASA TN D-2565, 1965.

27. Hilsenrath, Joseph; Beckett, Charles W.; Benedict, William S.; et al.: Tables of Thermal Properties of Gases Comprising Tables of Thermodynamic and Transport Properties of Air, Argon, Carbon Dioxide, Carbon Monoxide, Hydrogen, Nitrogen, Oxygen, and Steam. Circ. 564, National Bureau of Standards, 1955.

TABLE I. - PERTINENT AREA RATIOS[a]

Nozzle	Area ratio						Nozzle discharge coefficient (nominal), C_{D8}
	Boattail to maximum nozzle area, [b]A_β/A_m	Nozzle throat to maximum nozzle area, A_8/A_m	Chute to maximum nozzle area, A_{ch}/A_m	Plug to maximum nozzle area, A_{pl}/A_m	Geometric area ratio, $(AR)_{geo}$	Effective area ratio, $(AR)_{eff}$	
Supersonic Tunnel Association (STA)	0.740	0.250	-----	-----	----	----	0.987
36-Chute suppressor	.129	.248	0.309	0.322	2.29	2.31	.990

[a]All areas are areas projected on a plane normal to the nozzle axis (except A_8, which is the actual geometric throat area).

[b]A_β does not include ejector boattail area.

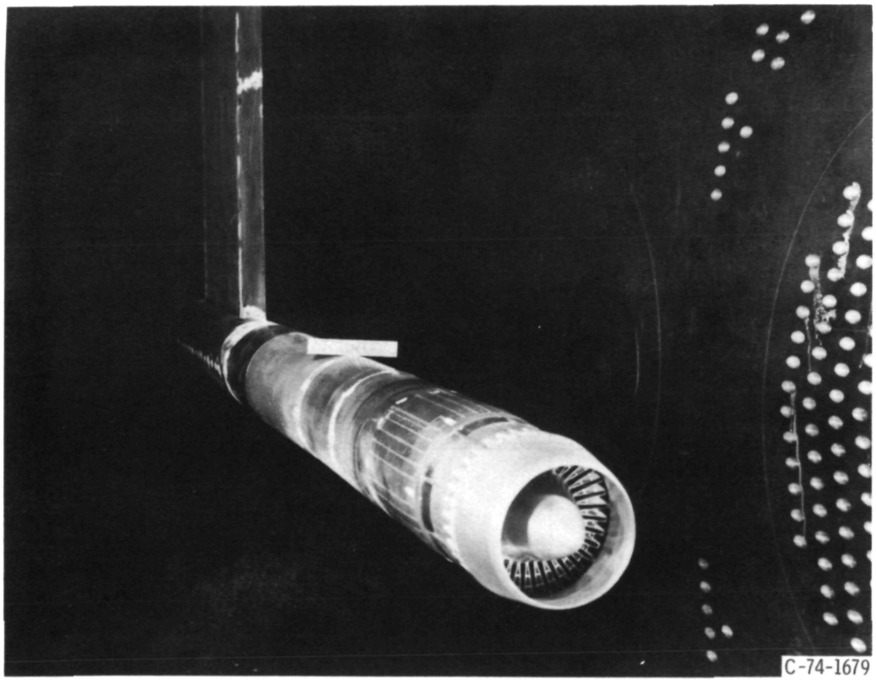

Figure 1. Model installed in 8- by 6-Foot Supersonic Wind Tunnel.

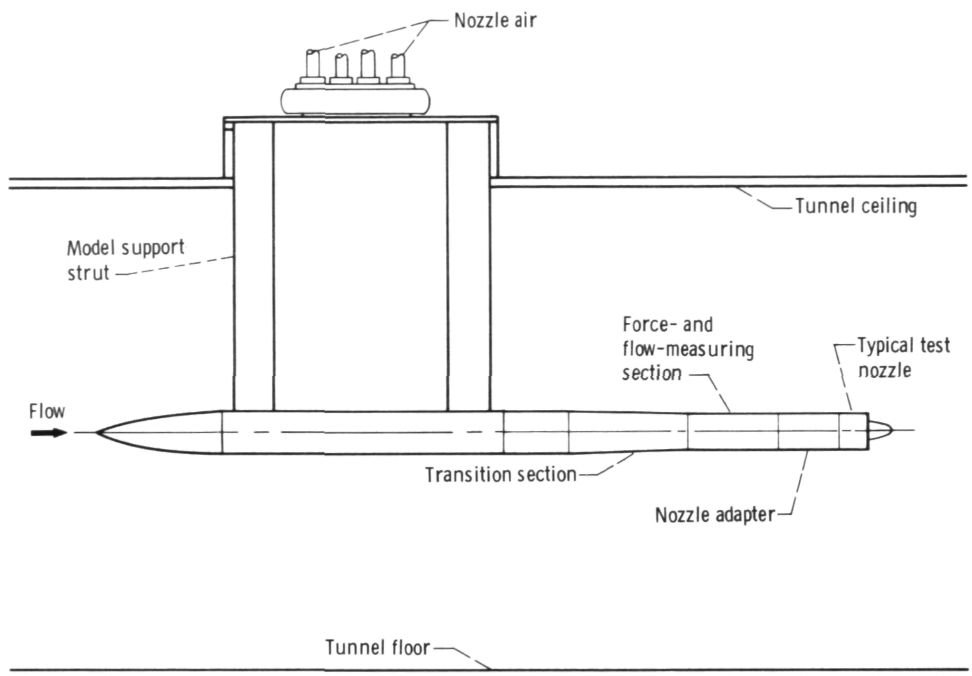

Figure 2. - Sketch of model installed in 8- by 6-Foot Supersonic Wind Tunnel.

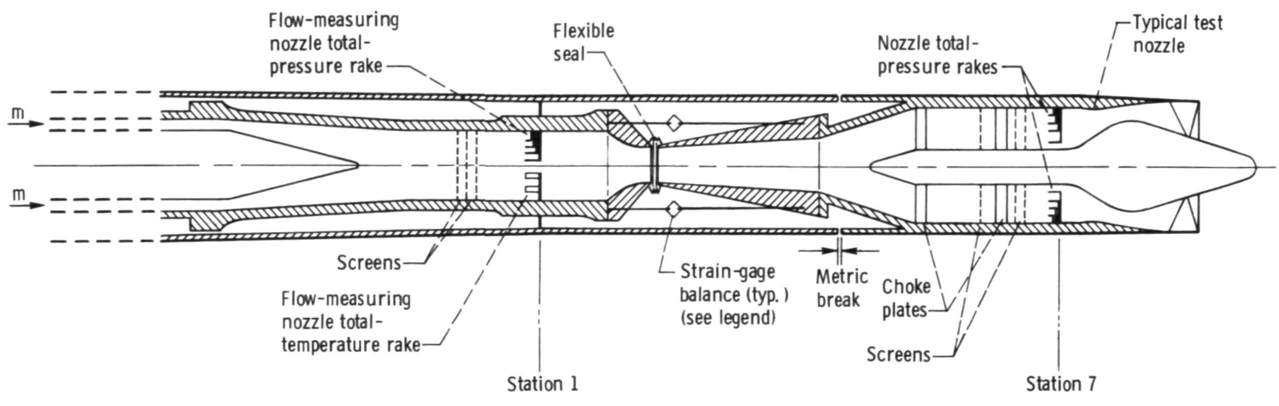

Figure 3. - Model internal geometry and thrust-measuring system. (Strain gages actually located at $\varphi = 90^0$ and $\varphi = 270^0$ ($\varphi = 0^0$ at top of model).)

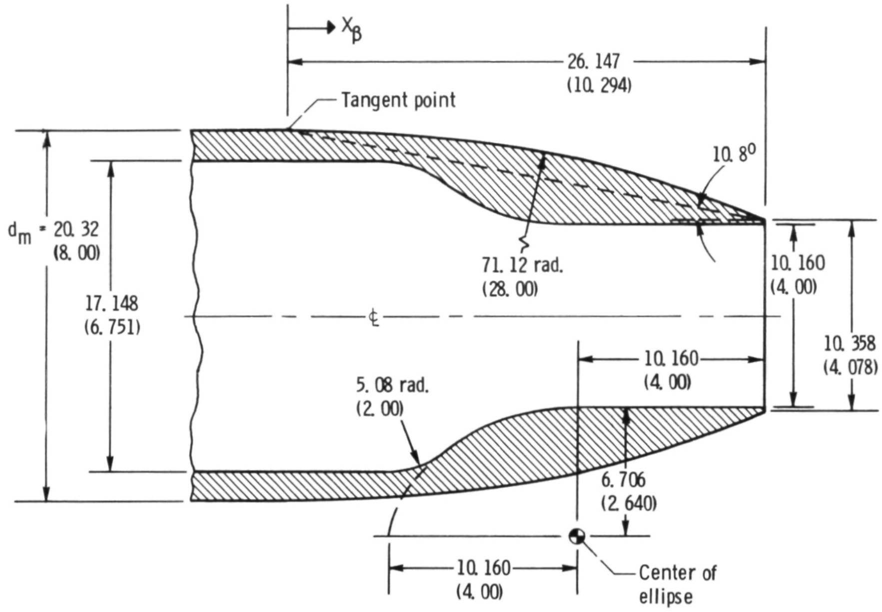

(a) Supersonic Tunnel Association (STA) nozzle.

Figure 4. - Geometric details of test nozzles. (All dimensions are in cm (in.).)

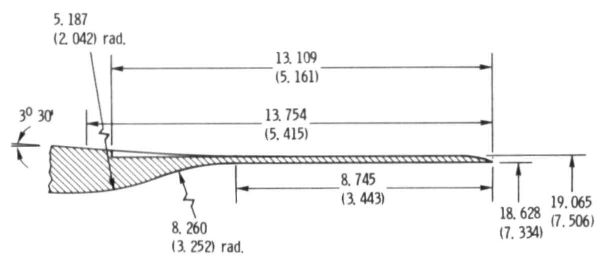

Shroud detail

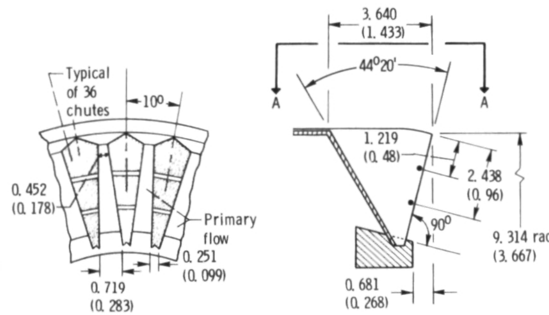

Chute detail

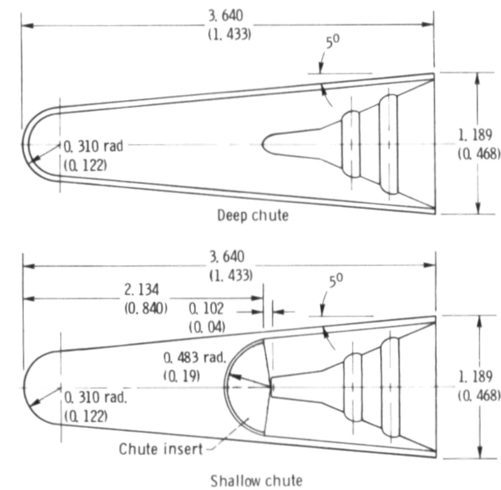

View A-A

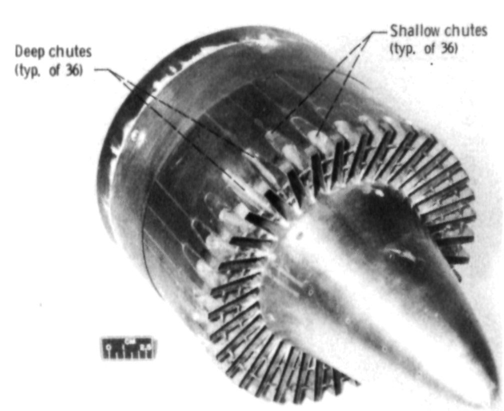

Z/d_m	r/d_m
0	0
.031	.058
.063	.081
.094	.100
.125	.115
.156	.128
.188	.140
.219	.151
.250	.162
.281	.171
.313	.180
.346	.190
.684	.280

} Straight line (last two rows)

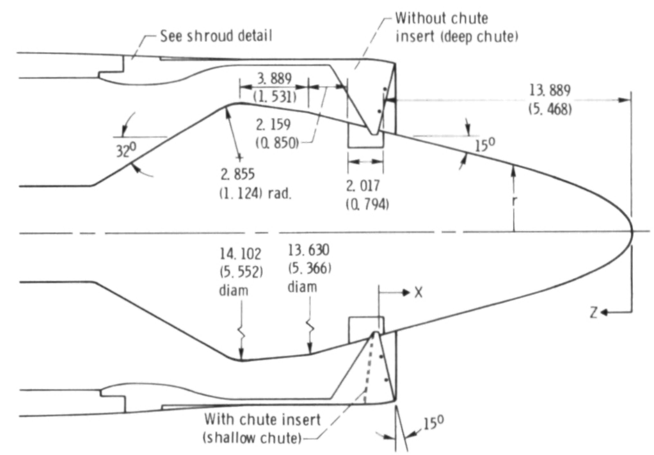

(b) Suppressor nozzles without an ejector.

Figure 4. - Continued.

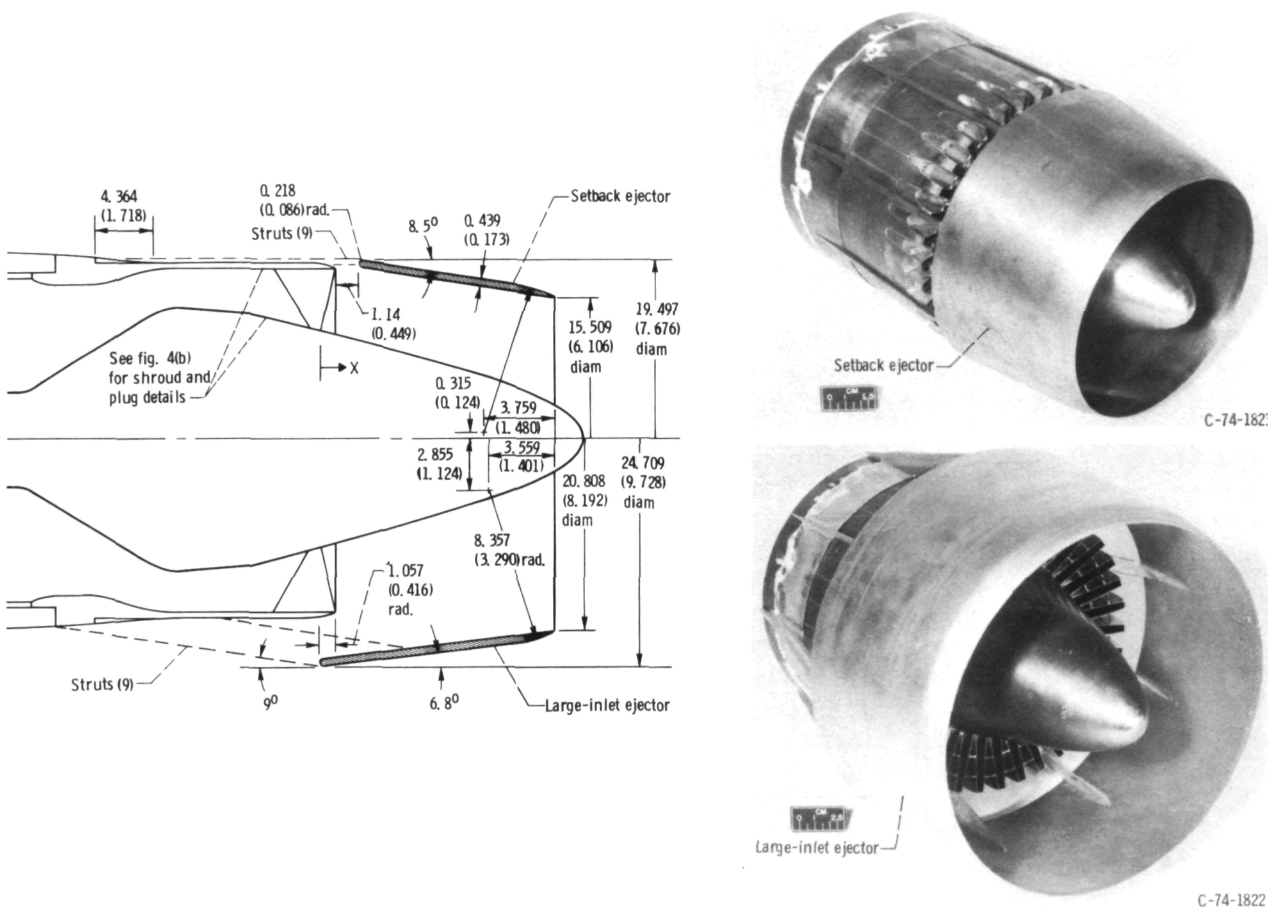

(c) Suppressor nozzles with two types of ejector.

Figure 4. - Concluded.

Orifice	Axial location, X_β/d_m	Circumferential location, φ deg
1	-0.167	90, 180, 270
2	0	↓
3	.193	↓
4	.373	↓
5	.566	↓
6	.746	↓
7	.927	↓
8	1.107	↓
9	1.197	↓
10	1.274	↓

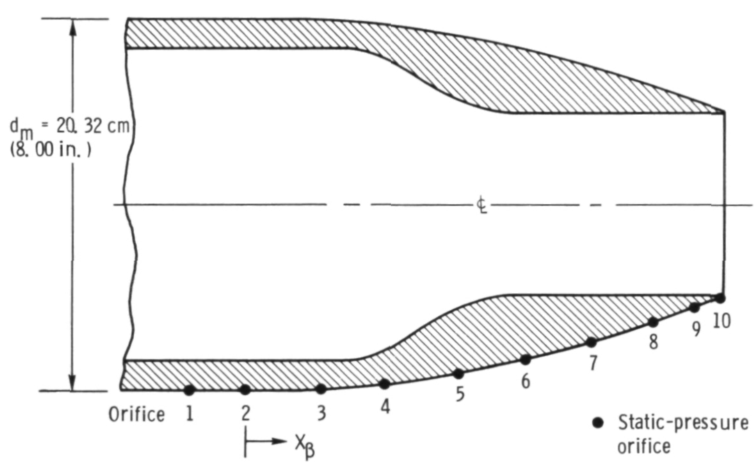

Figure 5. - Supersonic Tunnel Association (STA) boattail static-pressure instrumentation.

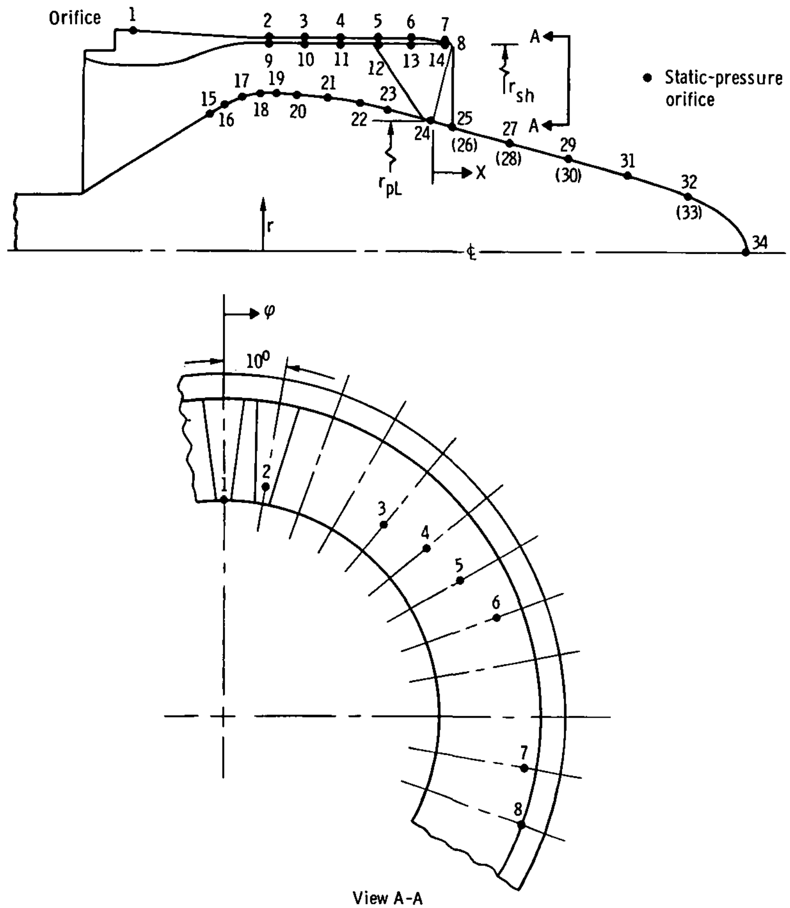

Orifice	Axial location, X/d_m	Circumferential location, φ, deg	Type of static pressure	Orifice	Axial location, X/d_m	Circumferential location, φ, deg	Type of static pressure
1	-0.653	315	External	18	-0.384	30	Plug
2	-.361	295		19	-.342		
3	-.280	275		20	-.300		
4	-.201	255		21	-.229		
5	-.122	235		22	-.157	7.5	
6	-.043	225		23	-.097	22.5	
7	.036	215		24	0	355	
8	.047	345		25	.040	7.5	
9	-.361	195	Internal	26	.040	0	
10	-.280	185		27	.172	7.5	
11	-.201	175		28	.172	0	
12	-.122	155		29	.303	7.5	
13	-.043	135		30	.303	0	
14	.036	115		31	.434	7.5	
15	-.496	30	Plug	32	.566	7.5	
16	-.459	30	Plug	33	.566	0	
17	-.421	30	Plug	34	.697	7.5	

Deep-chute base static pressures

Orifice	Radius parameter, R	Circumferential location, φ, deg
1	0.066	0
2	.266	10
3	.378	40
4	.490	50
5	.603	60
6	.727	70
7	.852	100
8	.977	110

Shallow-chute base static pressures

Orifice	Radius parameter, R	Circumferential location, φ, deg
1	0.050	0
2	.250	10
3	.385	40
4	.485	50
5	.591	60
6	.719	70
7	.834	100
8	.948	110

Figure 6. - Static-pressure instrumentation for suppressor nozzles. (Ejector shrouds were not instrumented.)

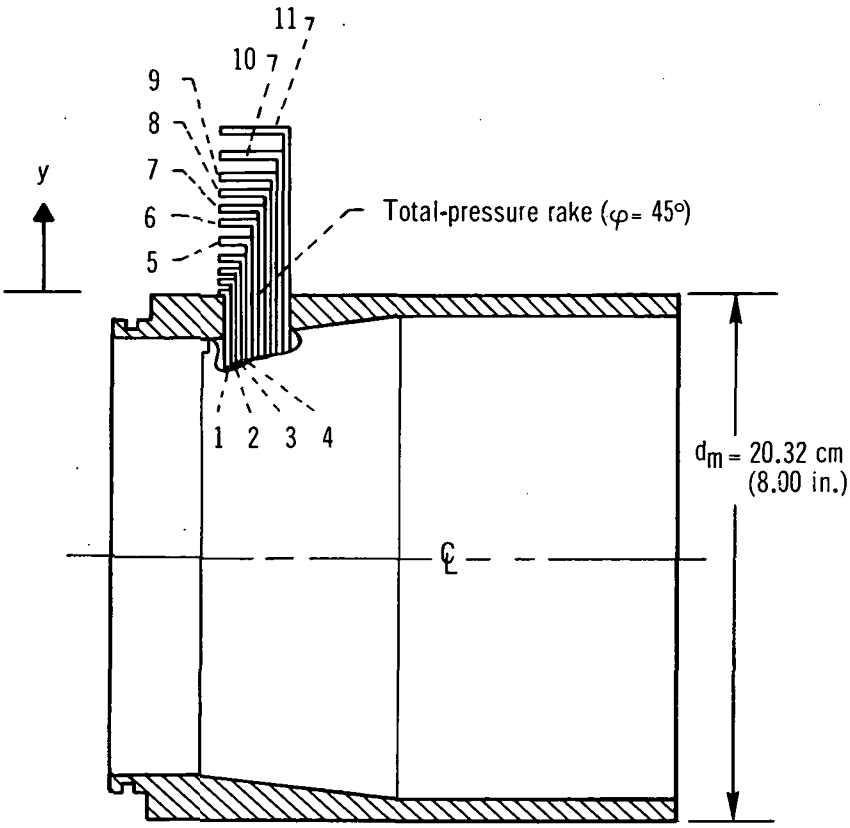

Tube	Tube location, y/d_m
1	0.009
2	.038
3	.047
4	.066
5	.075
6	.125
7	.150
8	.175
9	.200
10	.225
11	.250

Figure 7. - Boundary-layer shroud total-pressure tube locations. (Tubes located approximately 18 nozzle diameters downstream of nose.)

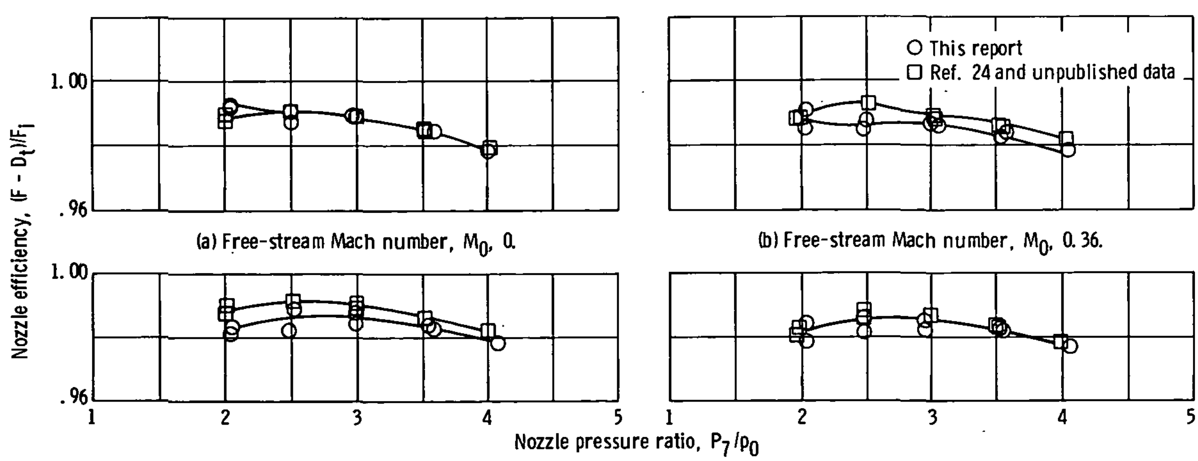

(c) Free-stream Mach number, M_0, 0.40.

(d) Free-stream Mach number, M_0, 0.45.

Figure 8. - Comparison of Supersonic Tunnel Association nozzle efficiencies from two tests.

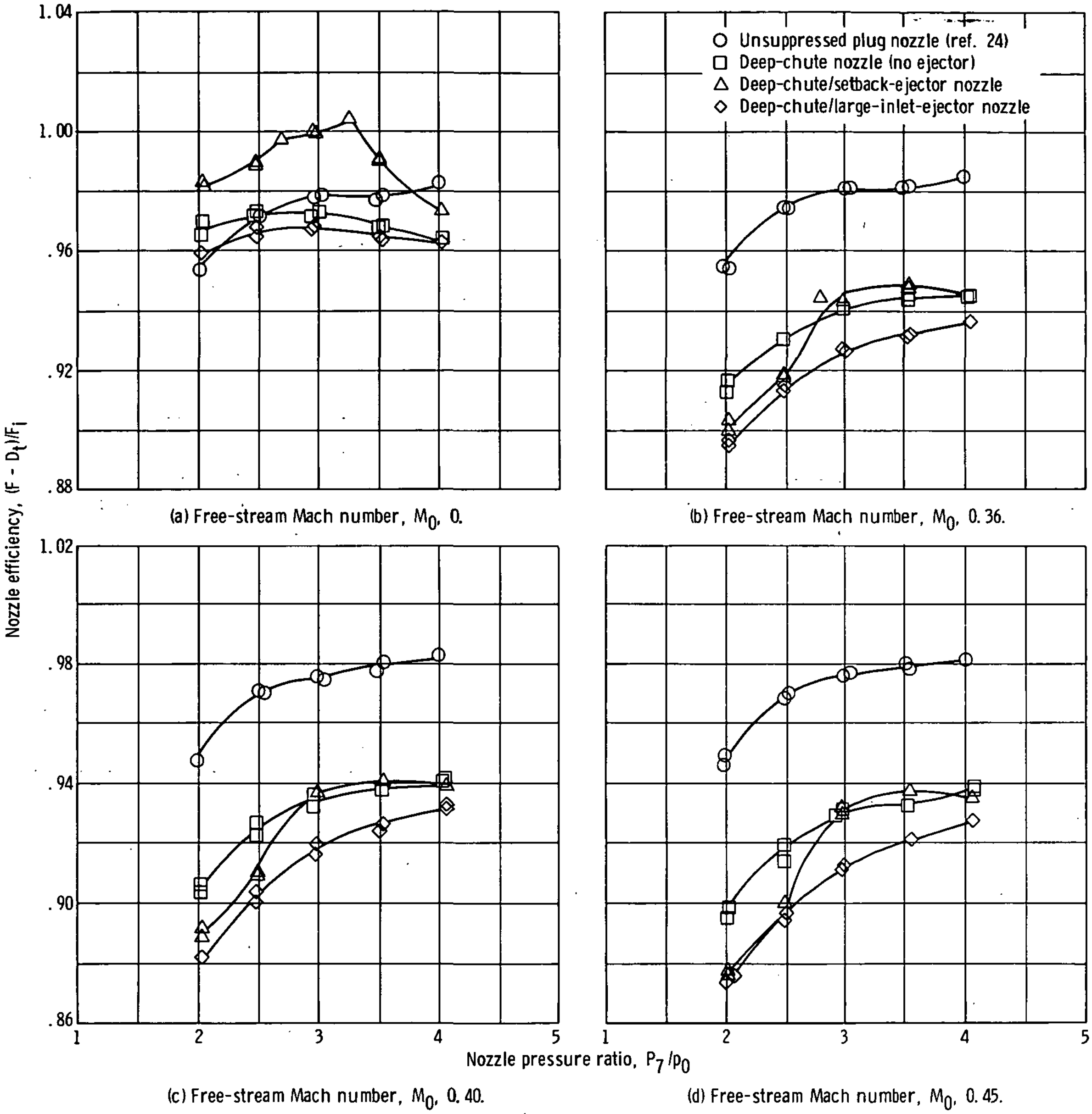

Figure 9. - Comparison of performance for unsuppressed plug nozzle and 36-deep-chute suppressor nozzle with and without ejector shrouds.

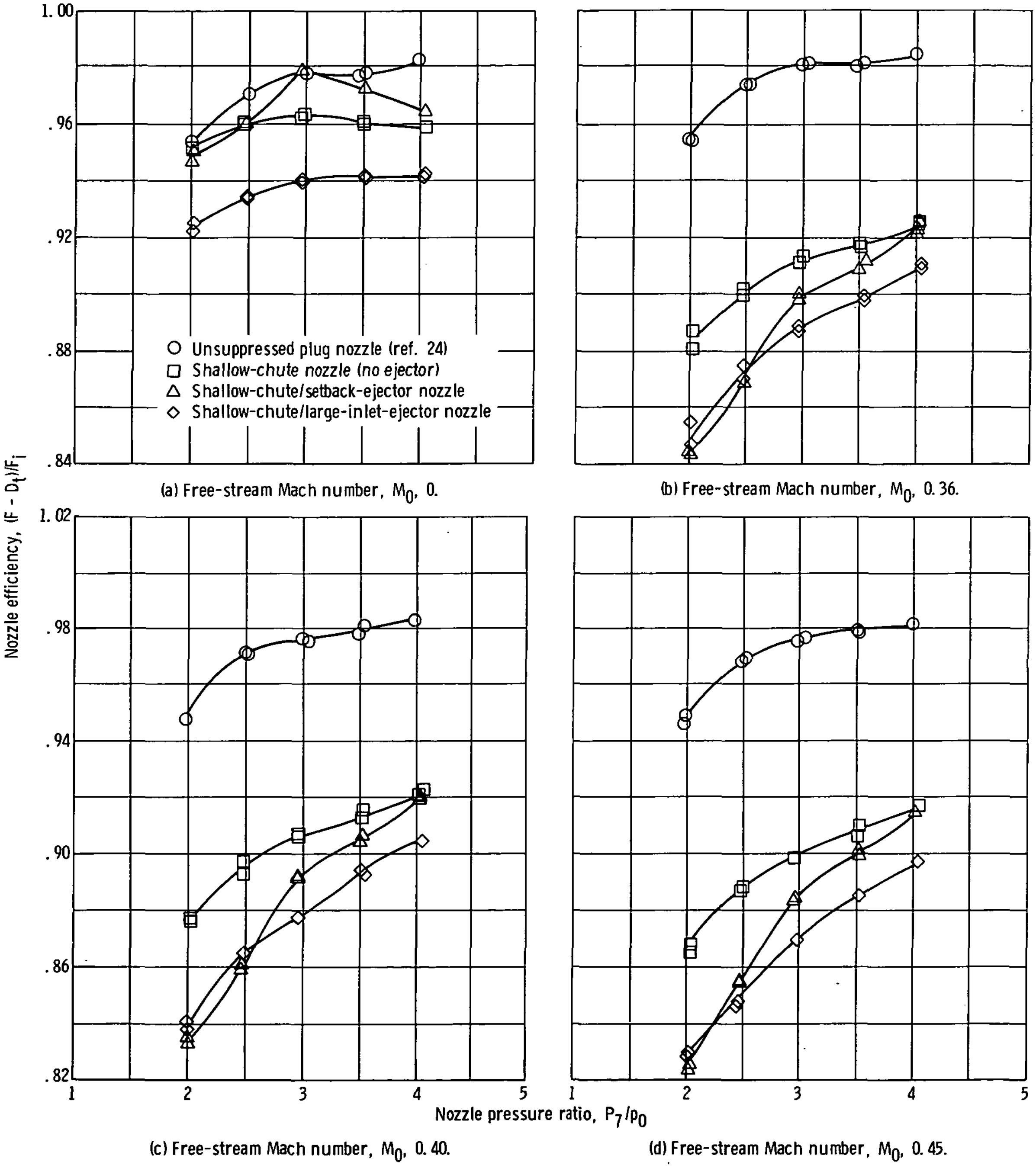

Figure 10. - Comparison of performance for unsuppressed plug nozzle and 36-shallow-chute suppressor nozzle with and without ejector shrouds.

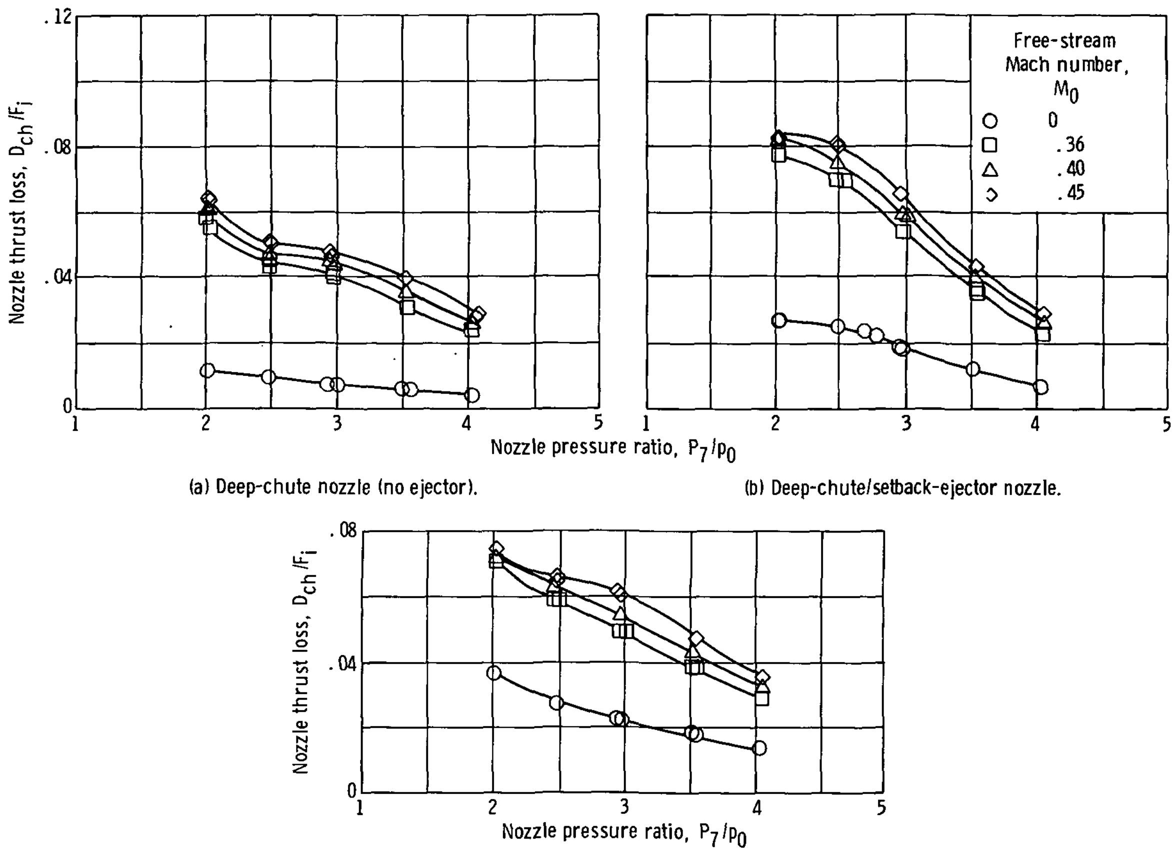

(a) Deep-chute nozzle (no ejector).

(b) Deep-chute/setback-ejector nozzle.

(c) Deep-chute/large-inlet-ejector nozzle.

Figure 11. - Nozzle thrust loss from chute-base pressure drag - deep-chute nozzles.

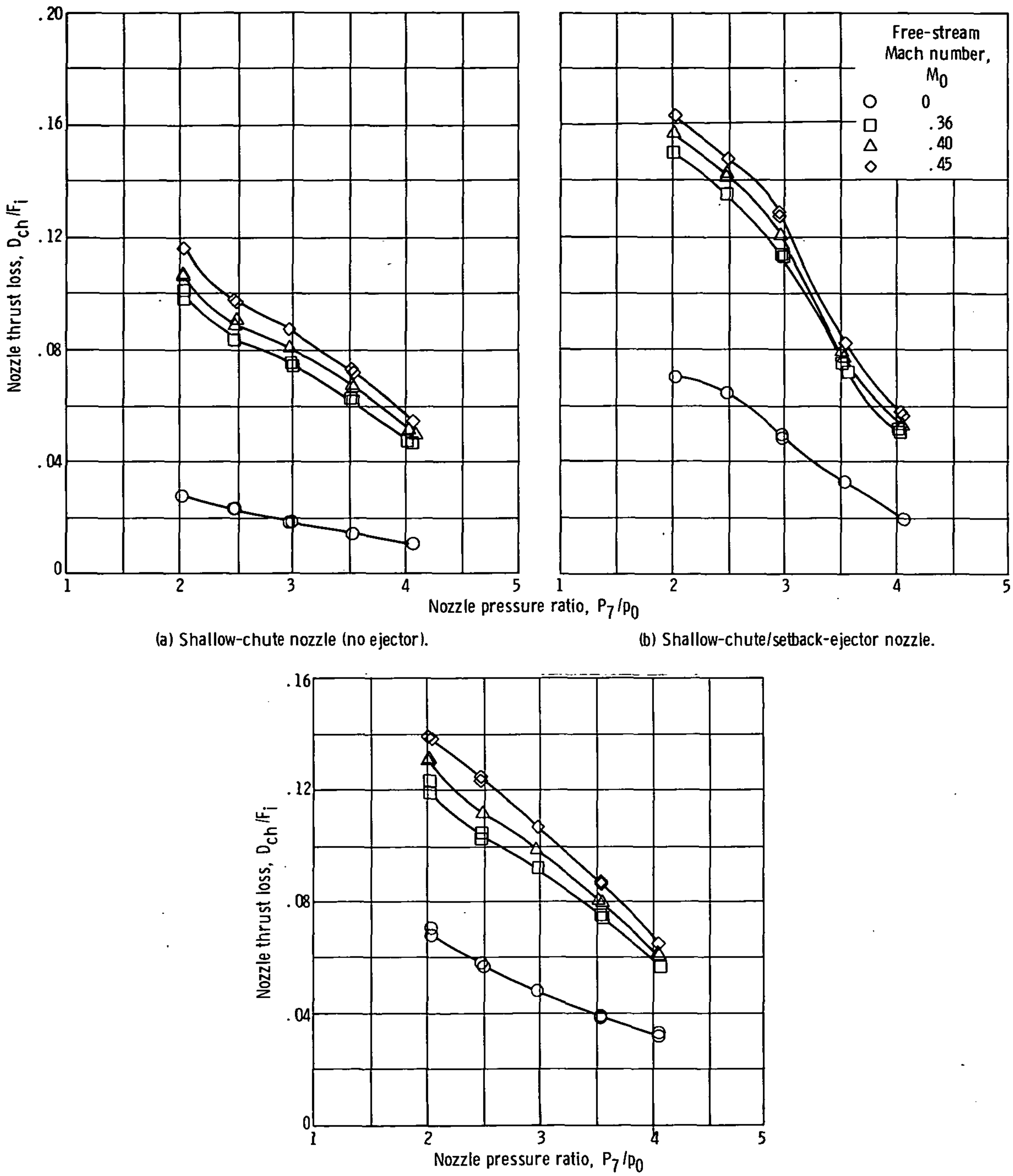

(a) Shallow-chute nozzle (no ejector).

(b) Shallow-chute/setback-ejector nozzle.

(c) Shallow-chute/large-inlet-ejector nozzle.

Figure 12. - Nozzle thrust loss from chute-base pressure drag - shallow-chute nozzles.

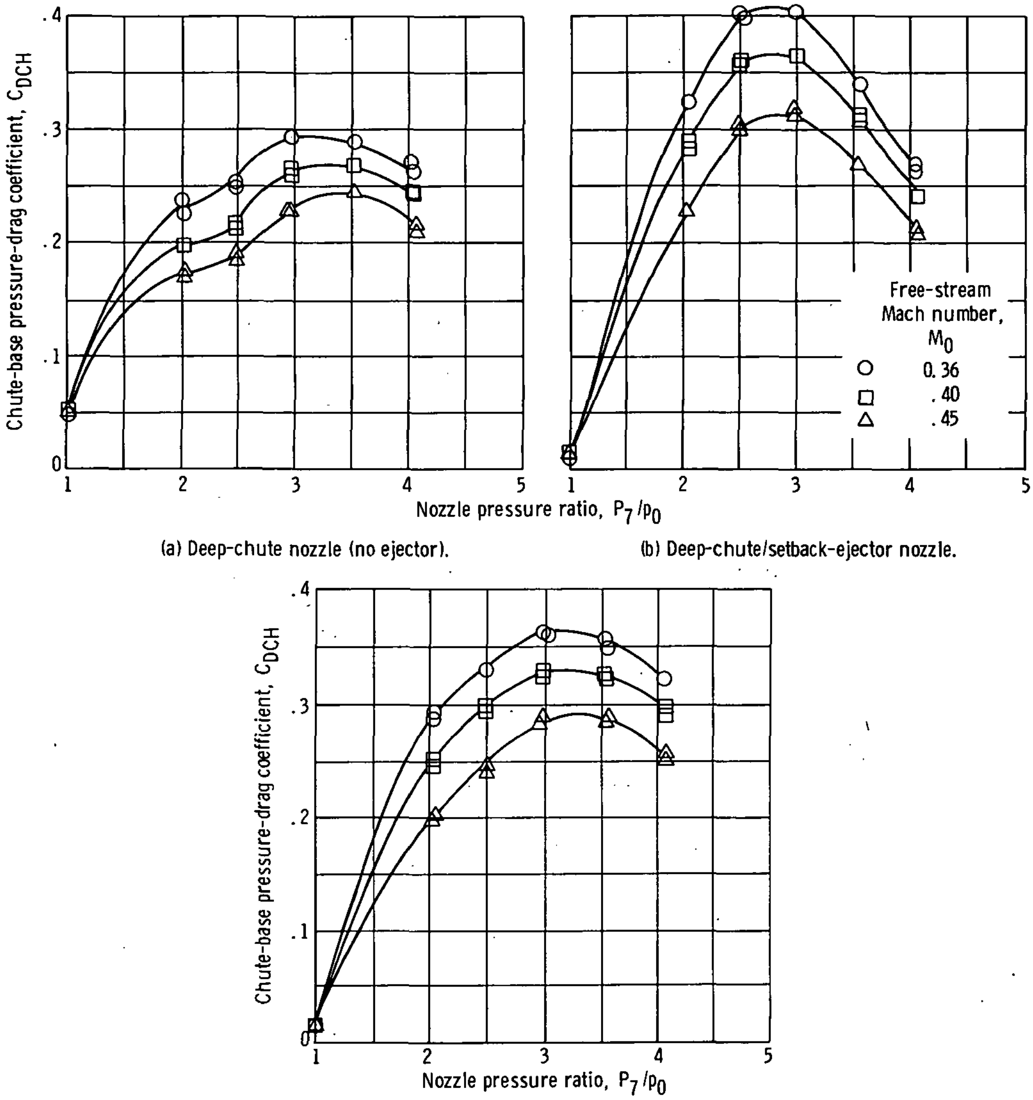

(a) Deep-chute nozzle (no ejector).

(b) Deep-chute/setback-ejector nozzle.

(c) Deep-chute/large-inlet-ejector nozzle.

Figure 13. - Chute-base pressure-drag coefficients of deep-chute suppressor nozzles.

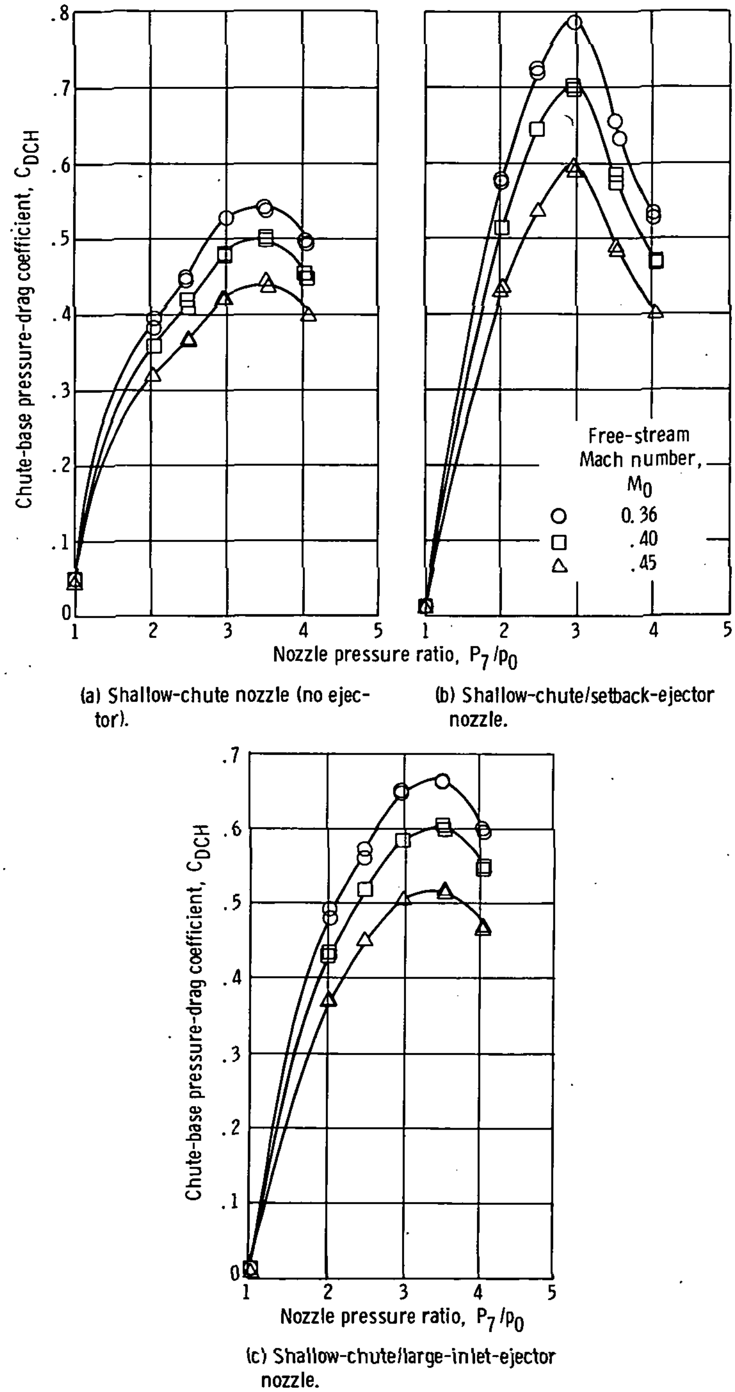

Figure 14. - Chute-base pressure-drag coefficients of shallow-chute suppressor nozzles.

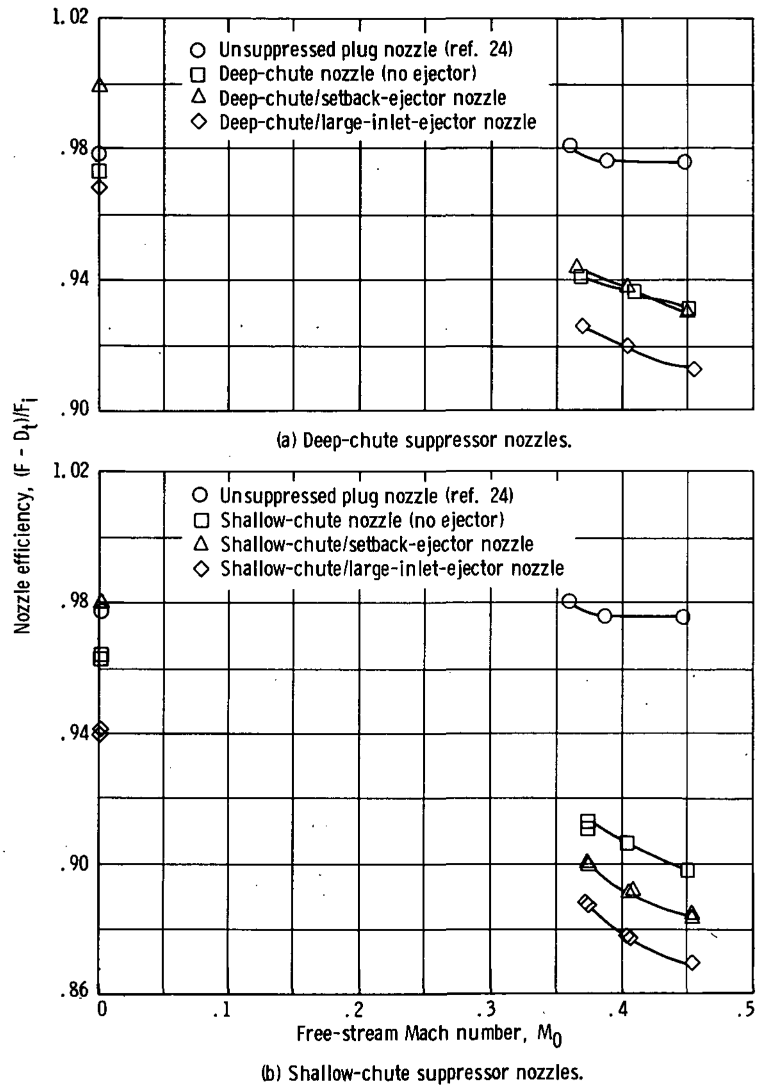

(b) Shallow-chute suppressor nozzles.

Figure 15. - External flow effects on nozzle performance of suppressor nozzles. Nozzle pressure ratio, P_7/p_0, 3.0.

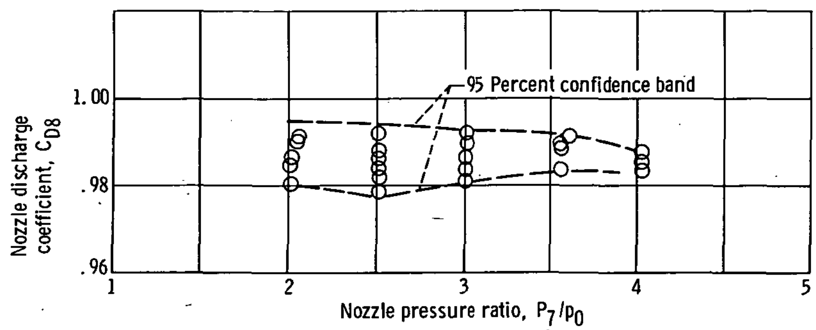

Figure 16. - Effect of nozzle pressure ratio on Supersonic Tunnel Association (STA) nozzle discharge coefficient. Free-stream Mach numbers, M_0, 0 to 0.45.

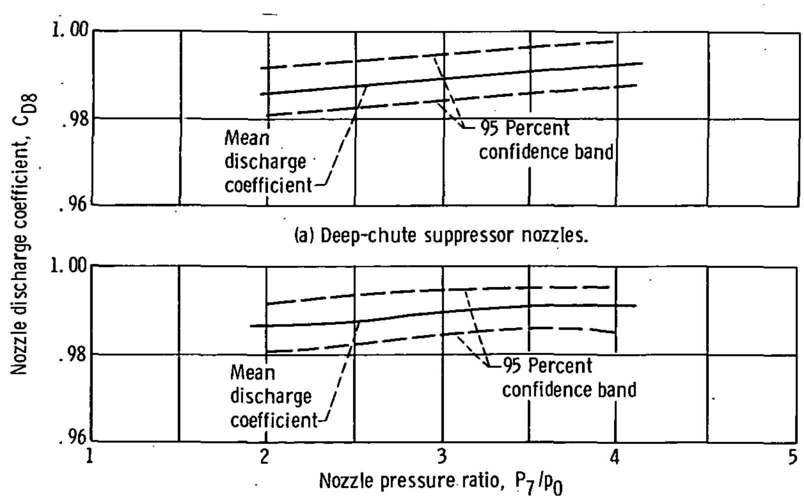

(a) Deep-chute suppressor nozzles.

(b) Shallow-chute suppressor nozzles.

Figure 17. - Effect of nozzle pressure ratio on suppressor nozzle discharge coefficient.

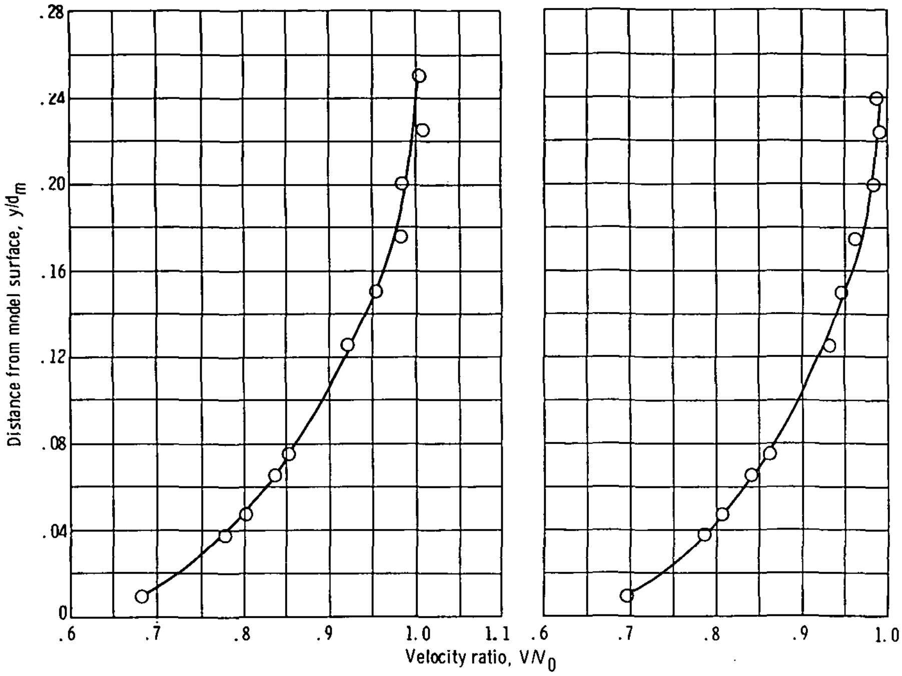

(a) Free-stream Mach number, M_0, 0.36; normalized boundary-layer displacement thickness, δ^*/d_m, 0.016; normalized boundary-layer momentum thickness, δ^{**}/d_m, 0.009.

(b) Free-stream Mach number, M_0, 0.40; normalized boundary-layer displacement thickness, δ^*/d_m, 0.015; normalized boundary-layer momentum thickness, δ^{**}/d_m, 0.008.

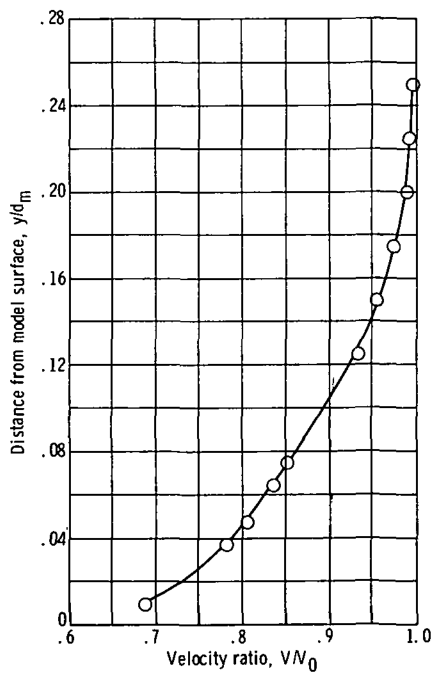

(c) Free-stream Mach number, M_0, 0.45; normalized boundary-layer displacement thickness, δ^*/d_m, 0.015; normalized momentum thickness, δ^{**}/d_m, 0.008.

Figure 18. - Boundary-layer velocity profiles at approximately 18 nozzle diameters from nose of model.

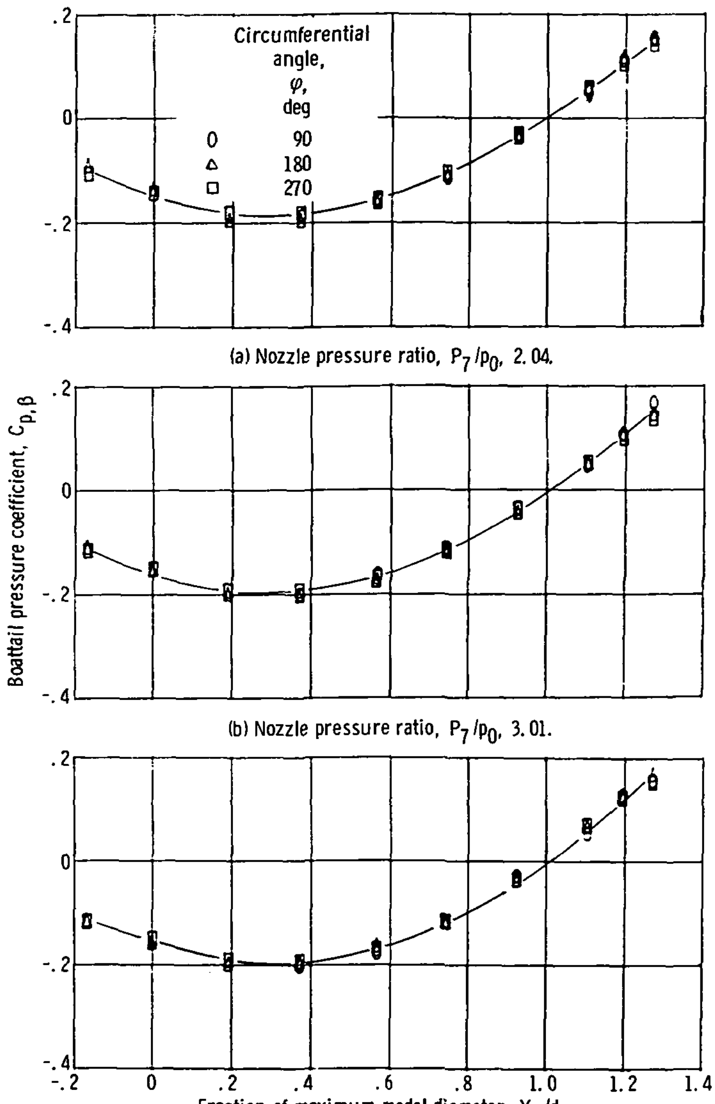

(a) Nozzle pressure ratio, P_7/p_0, 2.04.

(b) Nozzle pressure ratio, P_7/p_0, 3.01.

(c) Nozzle pressure ratio, P_7/p_0, 4.05.

Figure 19. - Supersonic Tunnel Association (STA) nozzle boattail pressure distributions. Free-stream Mach number, M_0, 0.36.

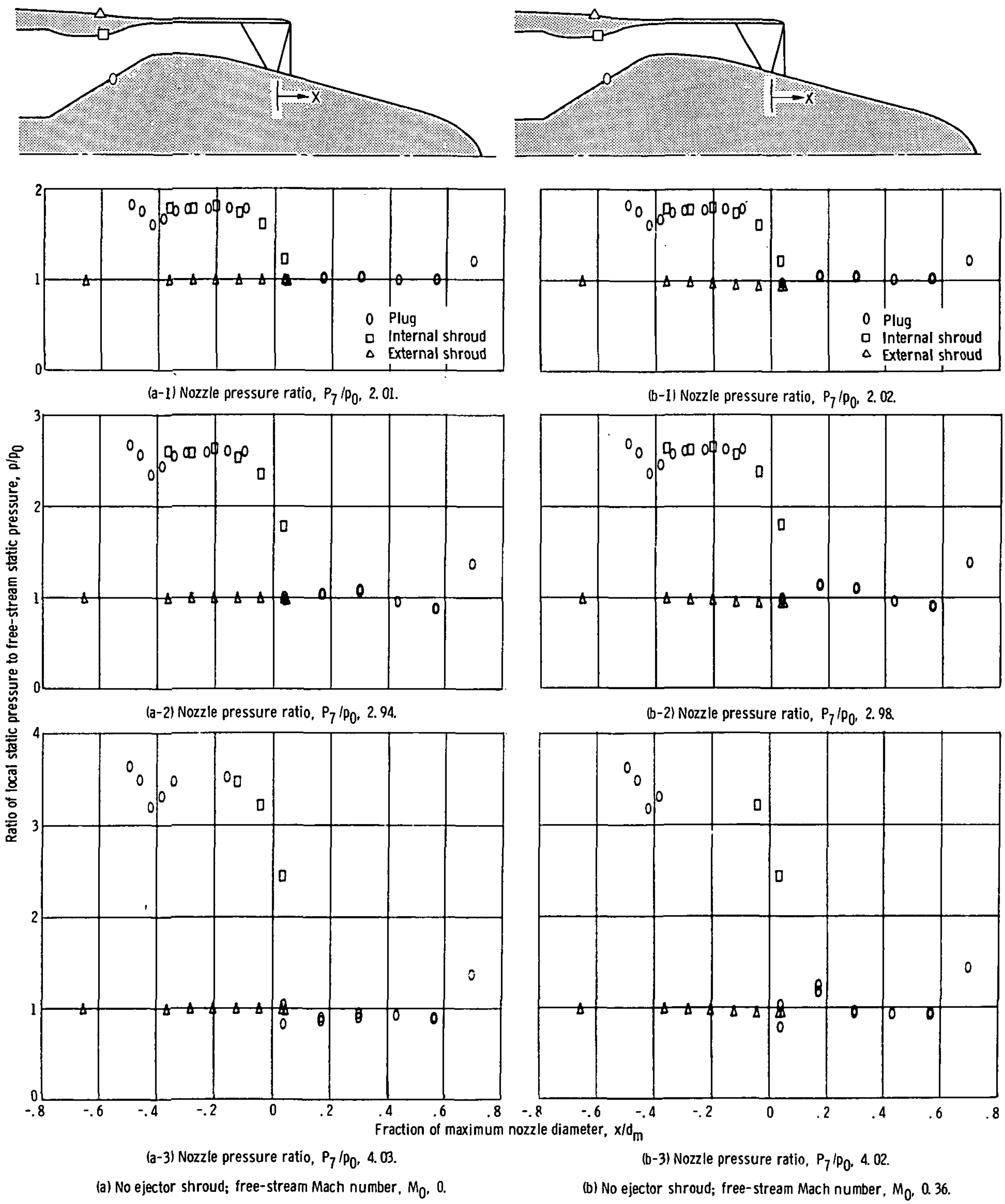

Figure 20. - Surface static-pressure distributions for deep-chute suppressor nozzles.

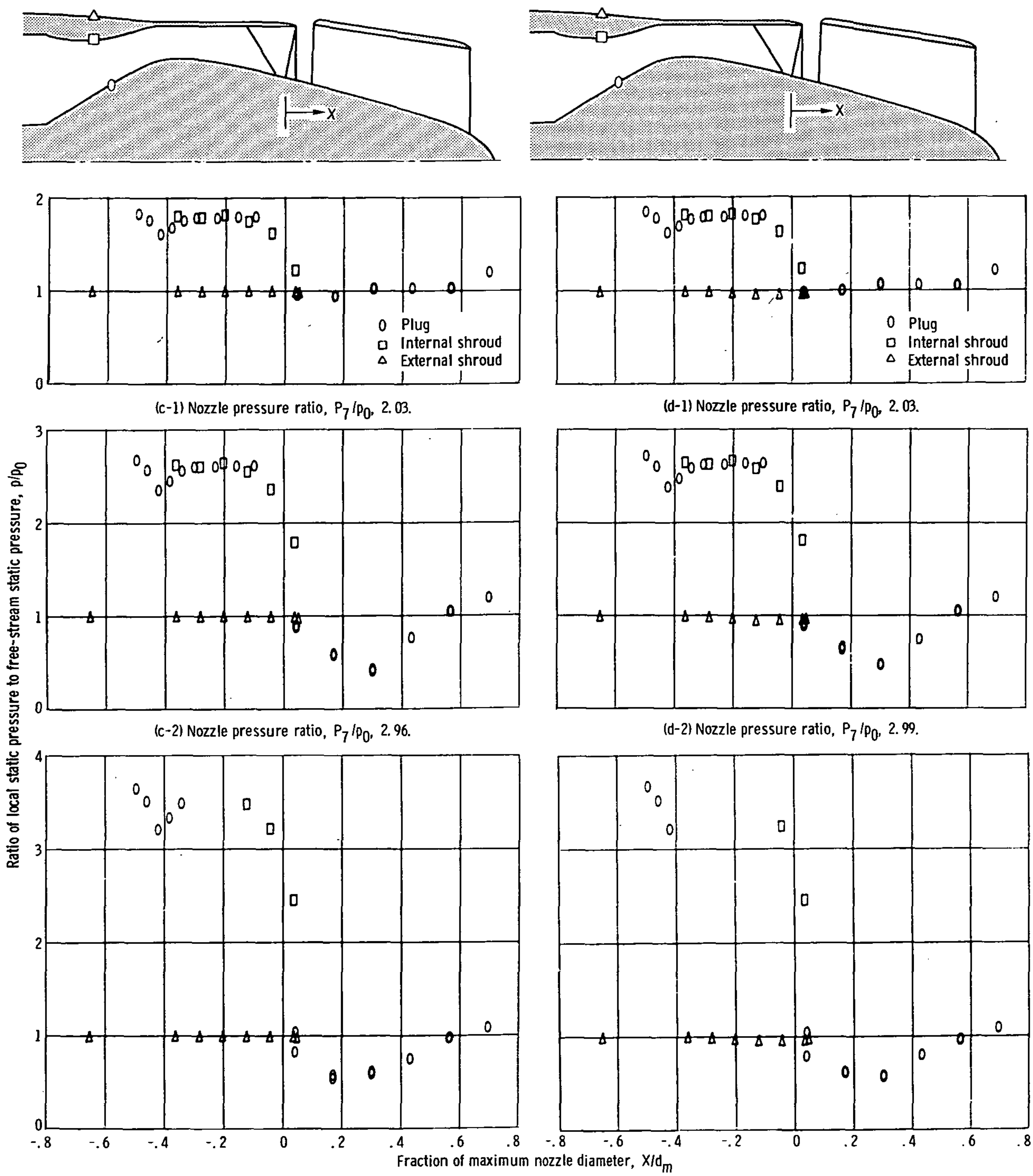

(c-1) Nozzle pressure ratio, P_7/p_0, 2.03.

(d-1) Nozzle pressure ratio, P_7/p_0, 2.03.

(c-2) Nozzle pressure ratio, P_7/p_0, 2.96.

(d-2) Nozzle pressure ratio, P_7/p_0, 2.99.

(c-3) Nozzle pressure ratio, P_7/p_0, 4.04.

(d-3) Nozzle pressure ratio, P_7/p_0, 4.05.

(c) With setback ejector; free-stream Mach number, M_0, 0.

(d) With setback ejector; free-stream Mach number, M_0, 0.36.

Figure 20. - Continued.

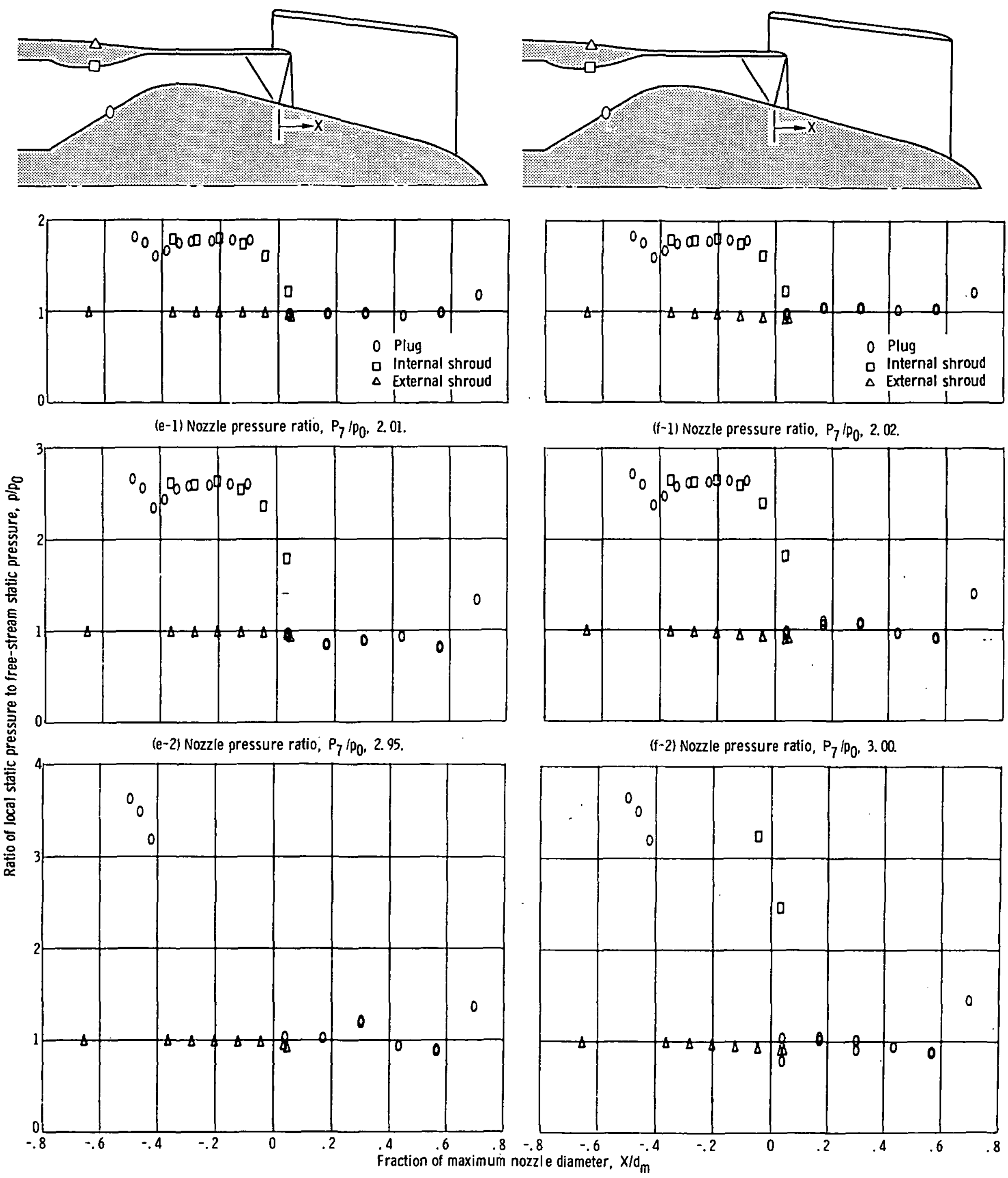

(e) With large-inlet ejector; free-stream Mach number, M_0, 0.

(f) With large-inlet ejector; free-stream Mach number, M_0, 0.36.

Figure 20. - Concluded.

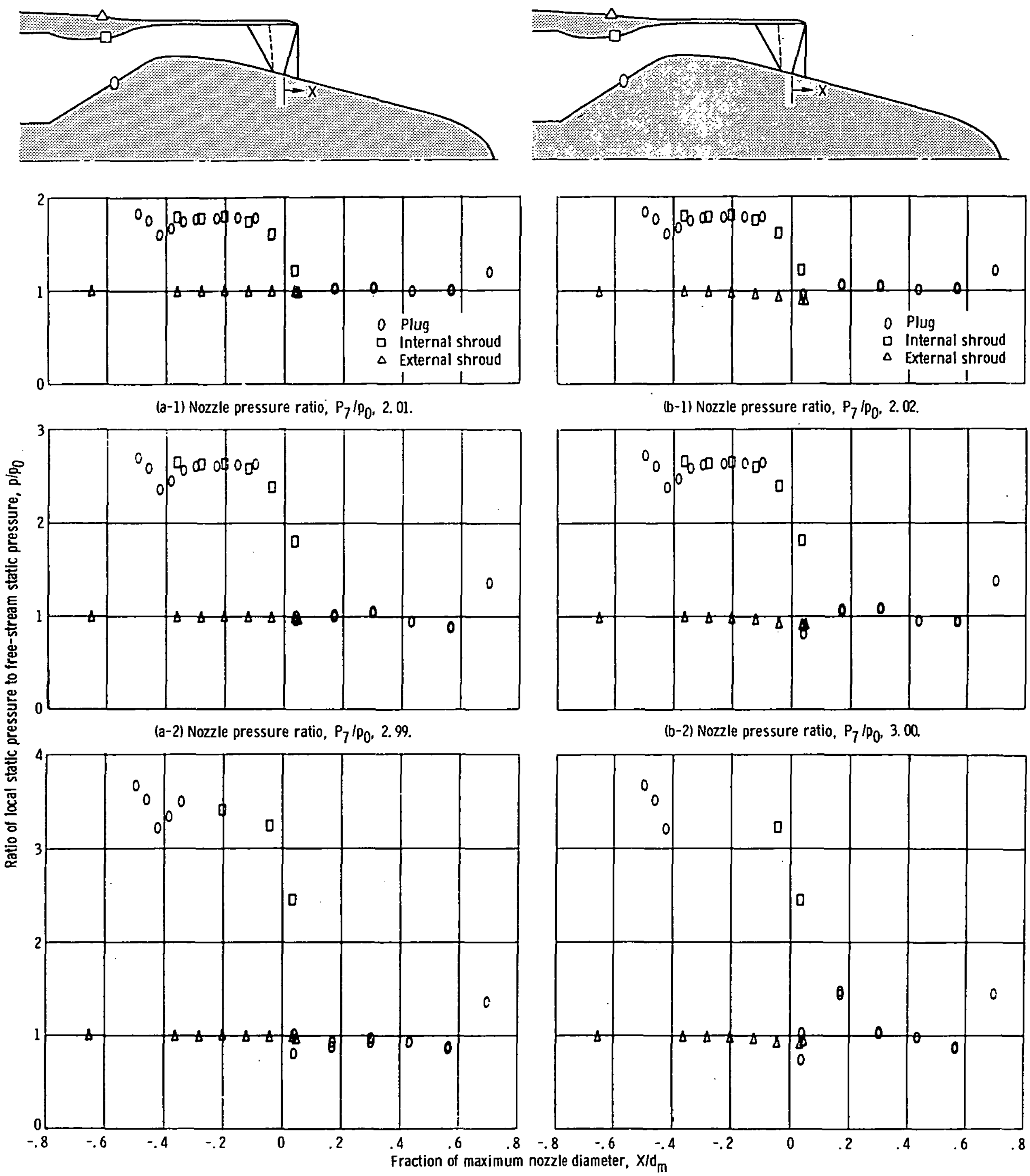

(a-1) Nozzle pressure ratio, P_7/p_0, 2.01.

(a-2) Nozzle pressure ratio, P_7/p_0, 2.99.

(a-3) Nozzle pressure ratio, P_7/p_0, 4.06.

(a) No ejector shroud; free-stream Mach number, M_0, 0.

(b-1) Nozzle pressure ratio, P_7/p_0, 2.02.

(b-2) Nozzle pressure ratio, P_7/p_0, 3.00.

(b-3) Nozzle pressure ratio, P_7/p_0, 4.04.

(b) No ejector shroud; free-stream Mach number, M_0, 0.36.

Figure 21. - Surface static-pressure distributions for shallow-chute suppressor nozzles.

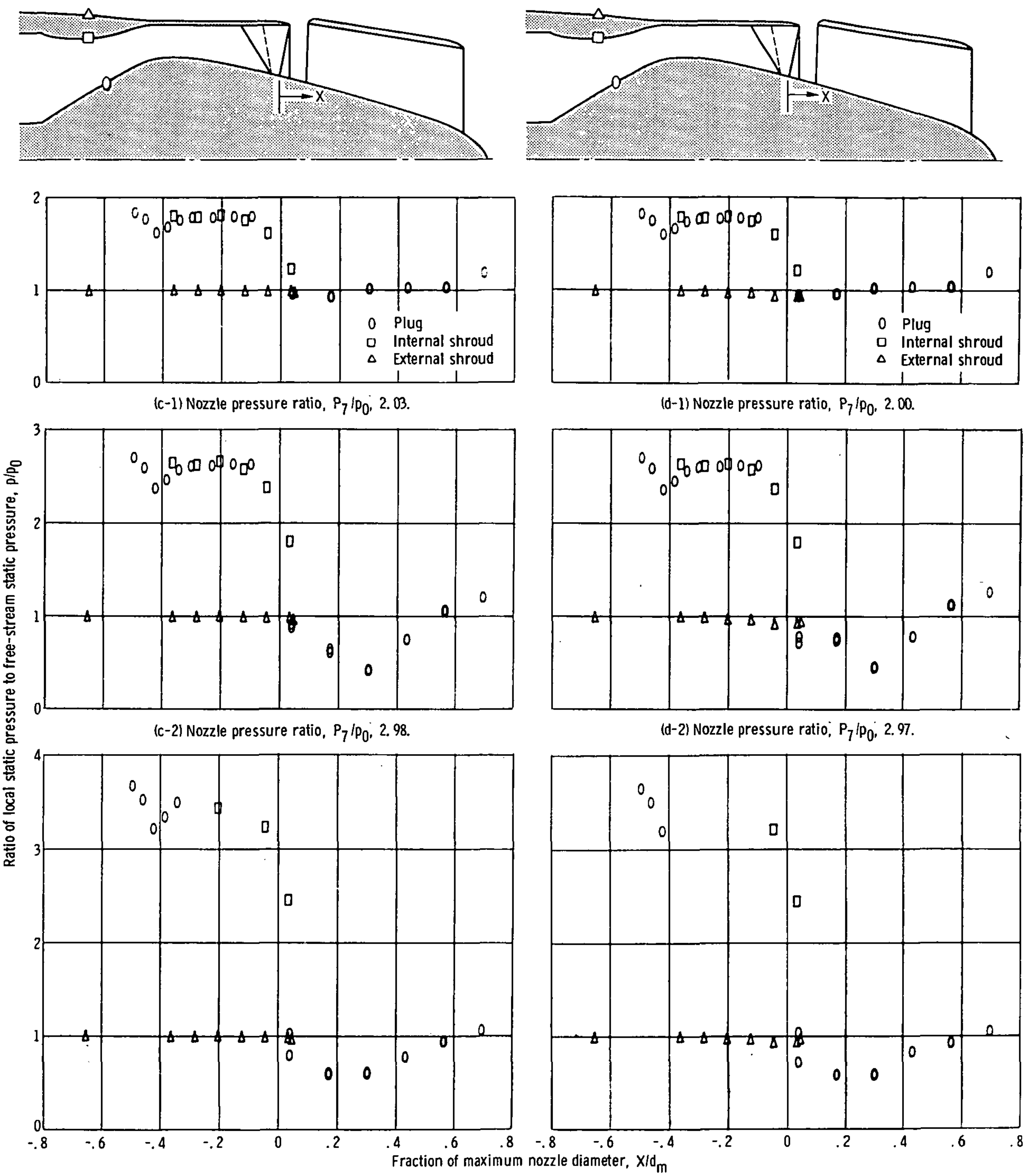

(c-1) Nozzle pressure ratio, P_7/p_0, 2.03.

(d-1) Nozzle pressure ratio, P_7/p_0, 2.00.

(c-2) Nozzle pressure ratio, P_7/p_0, 2.98.

(d-2) Nozzle pressure ratio, P_7/p_0, 2.97.

(c-3) Nozzle pressure ratio, P_7/p_0, 4.06.

(d-3) Nozzle pressure ratio, P_7/p_0, 4.03.

(c) With setback ejector; free-stream Mach number, M_0, 0.

(d) With setback ejector; free-stream Mach number, M_0, 0.36

Figure 21. - Continued.

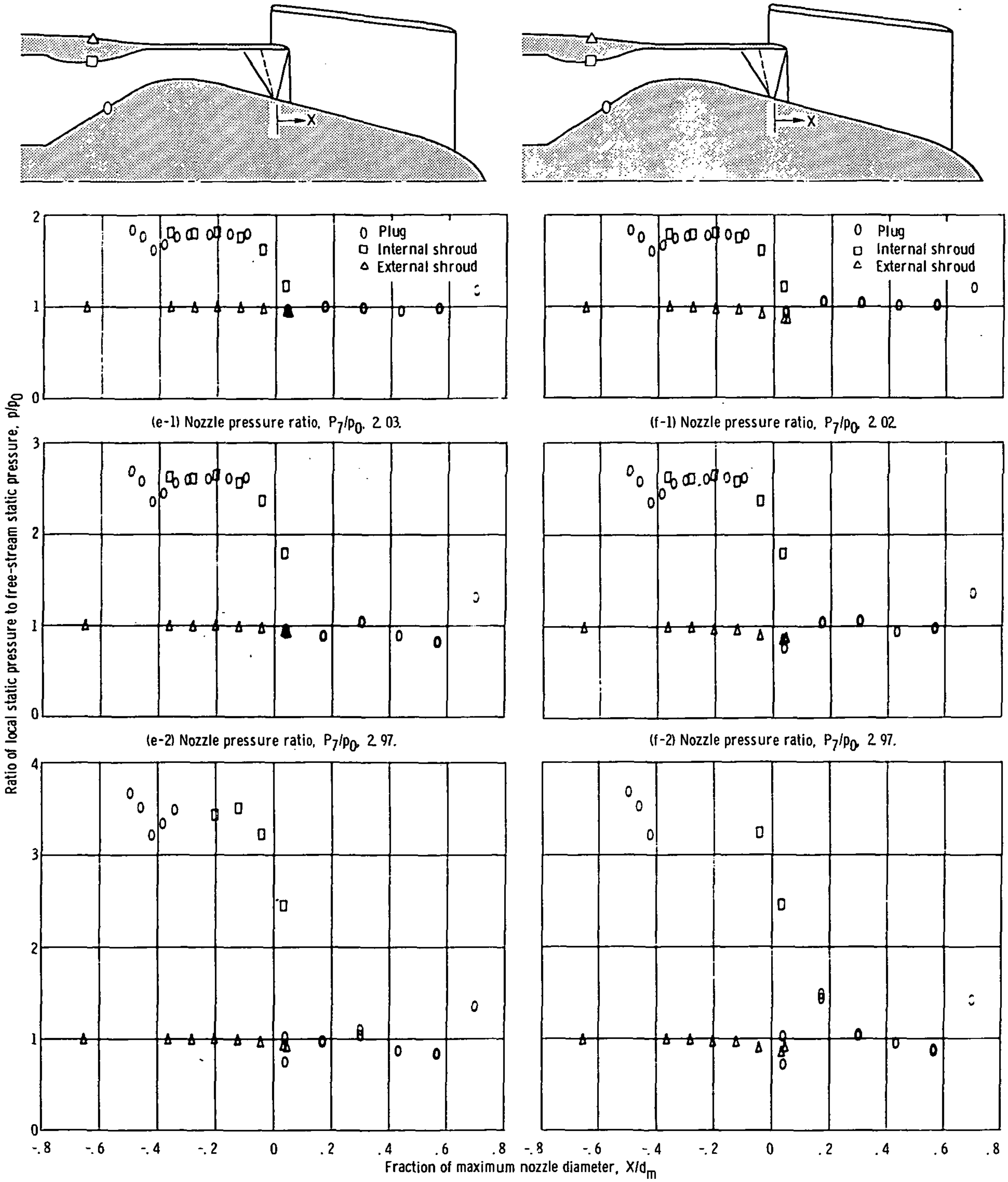

(e-3) Nozzle pressure ratio, P_7/p_0, 4.05.

(e) With large-inlet ejector; free-stream Mach number, M_0, 0.

(f-3) Nozzle pressure ratio, P_7/p_0, 4.06.

(f) With large-inlet ejector; free-stream Mach number, M_0, 0.36.

Figure 21. - Concluded.

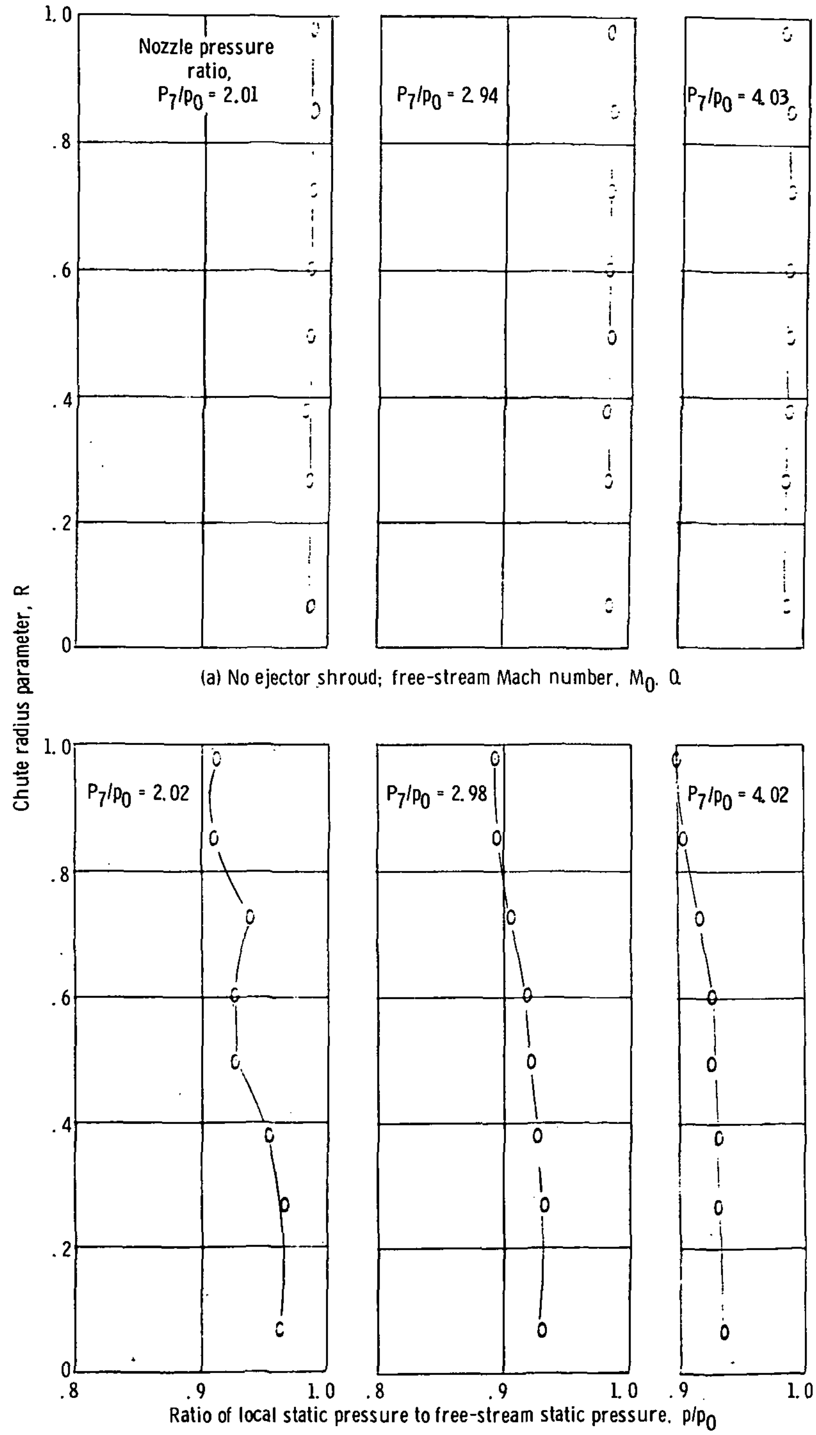

(a) No ejector shroud; free-stream Mach number, M_0, 0.

(b) No ejector shroud; free-stream Mach number, M_0, 0.36.

Figure 22. - Chute-base static-pressure distributions for deep-chute suppressor nozzles.

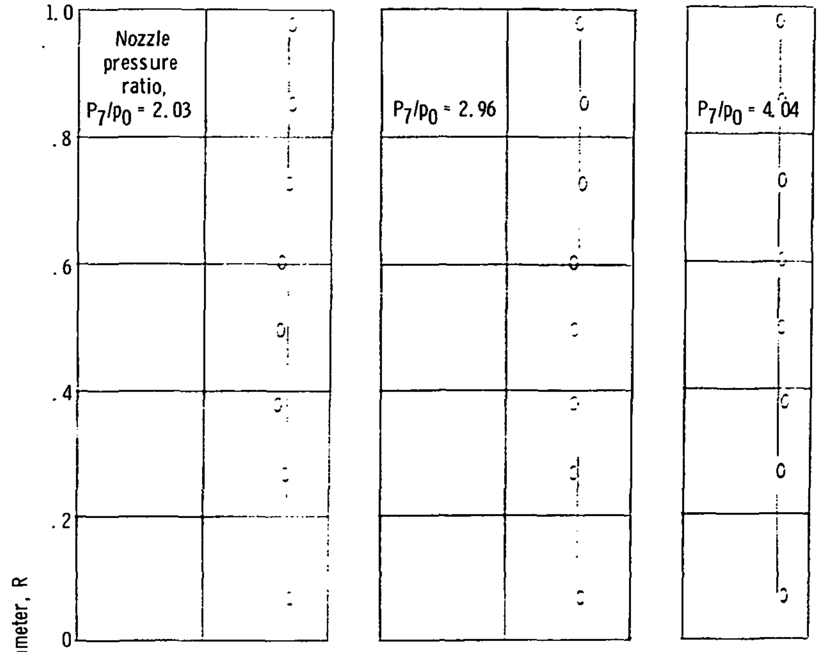

(c) With setback ejector; free-stream Mach number, M_0, 0.

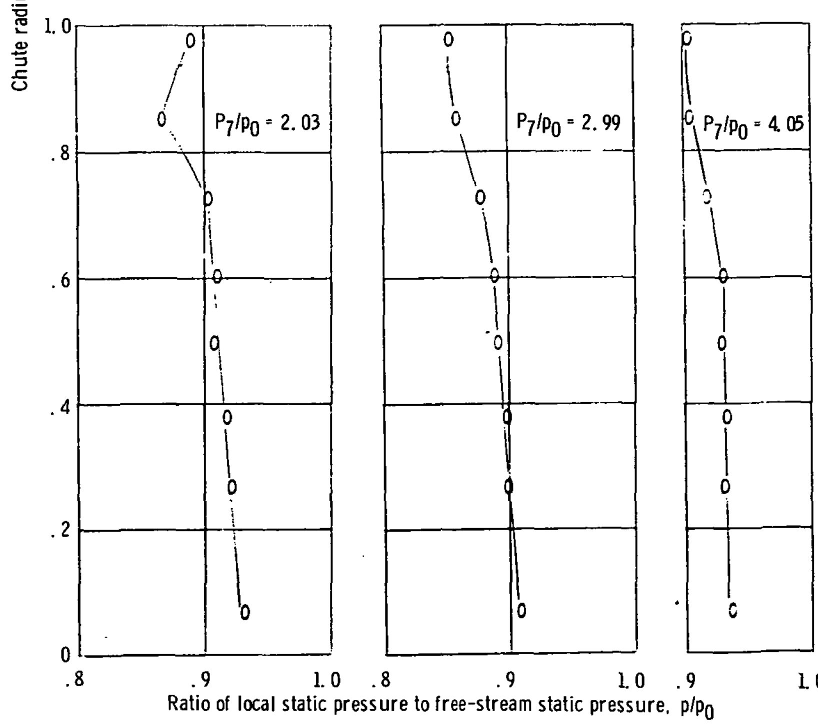

(d) With setback ejector; free-stream Mach number, M_0, 0.36.

Figure 22. - Continued.

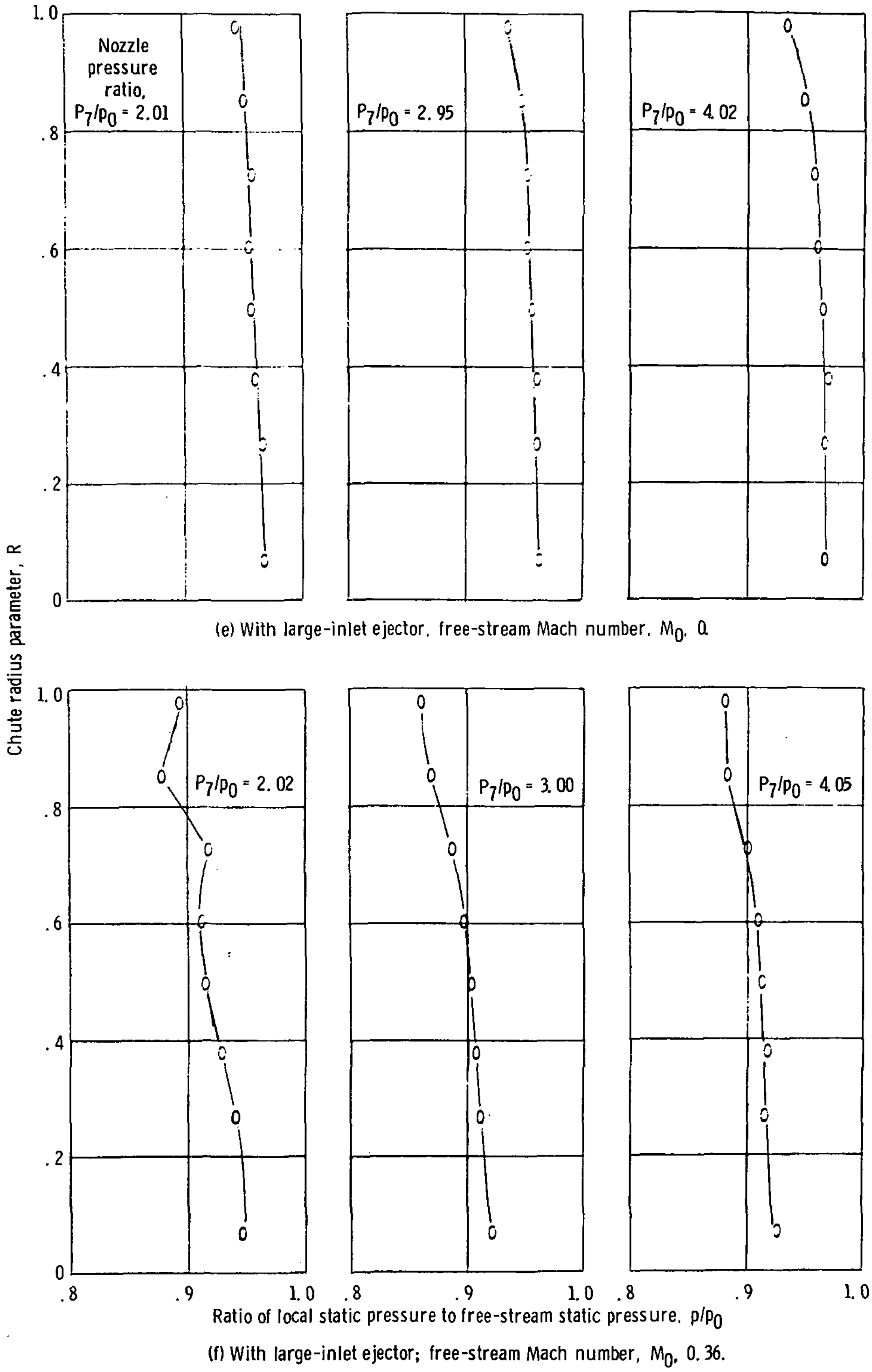

(f) With large-inlet ejector; free-stream Mach number, M_0, 0.36.

Figure 22. - Concluded.

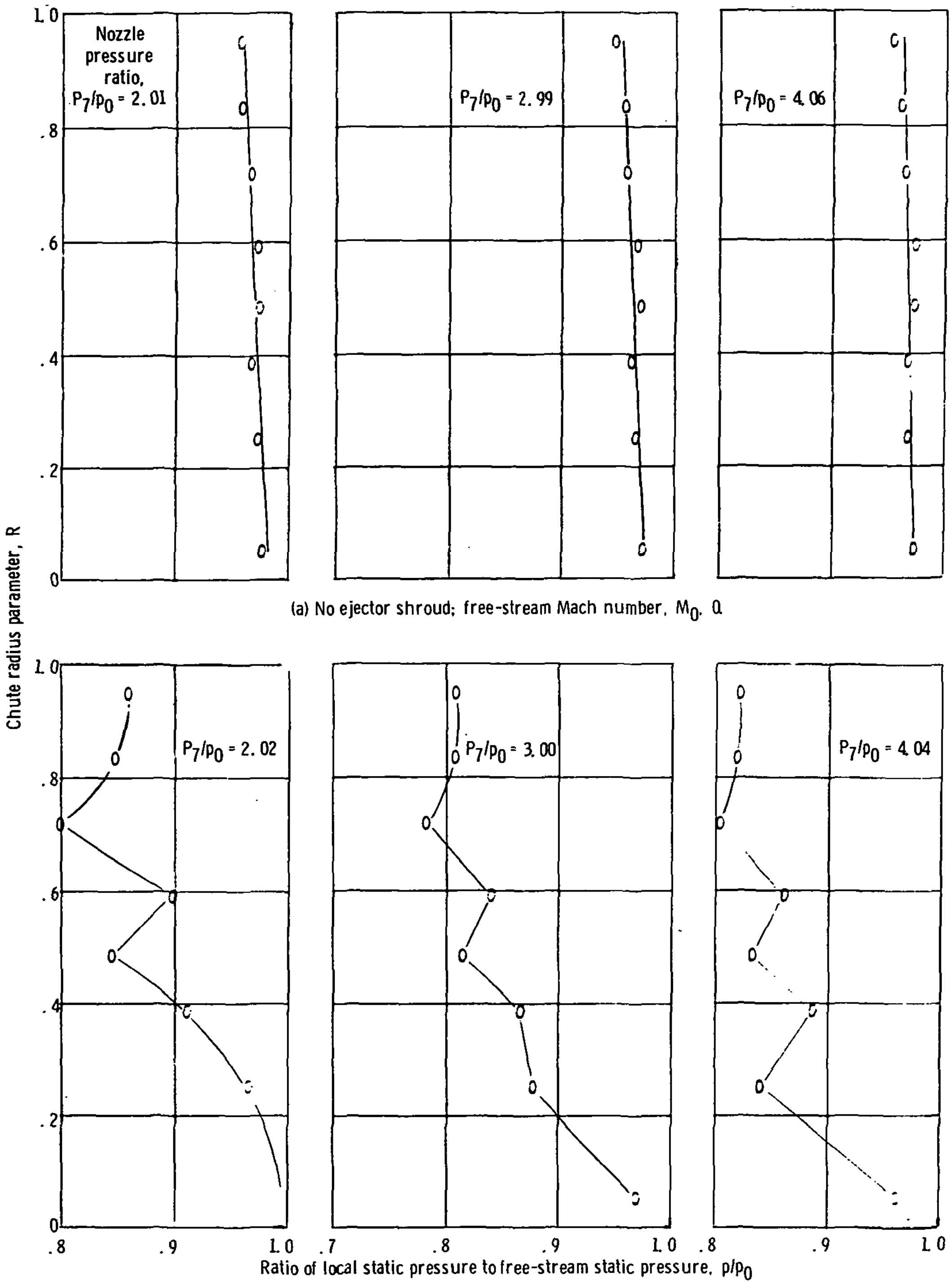

Figure 23. - Chute-base static-pressure distributions for shallow-chute suppressor nozzles.

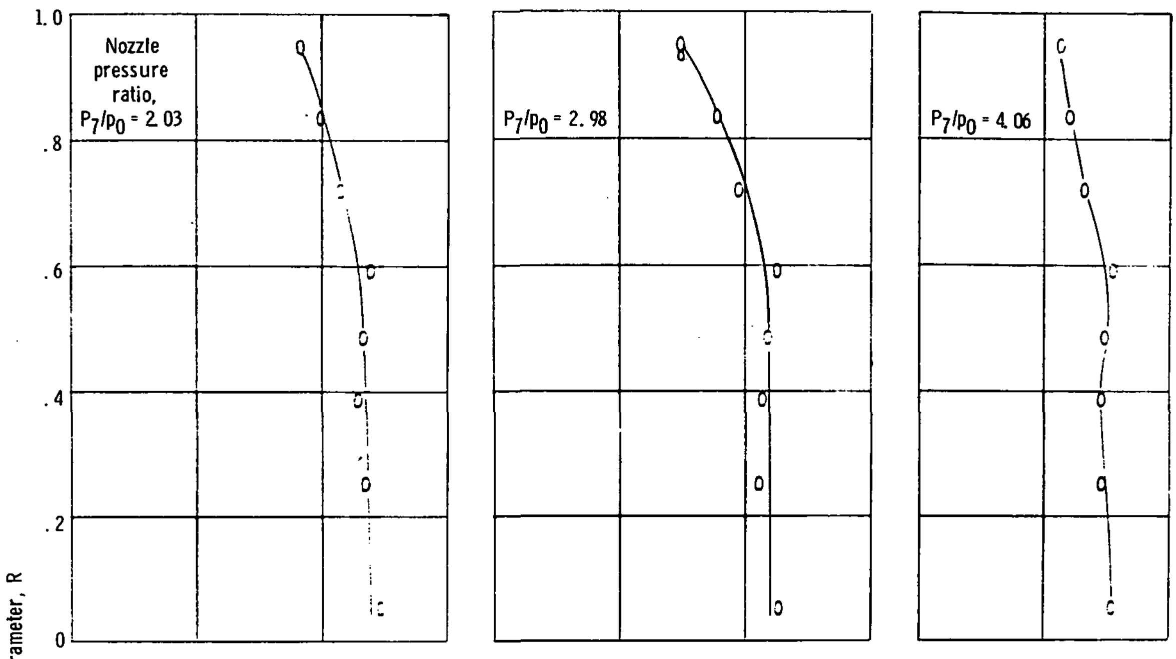

(c) With setback ejector; free-stream Mach number, M_0, 0.

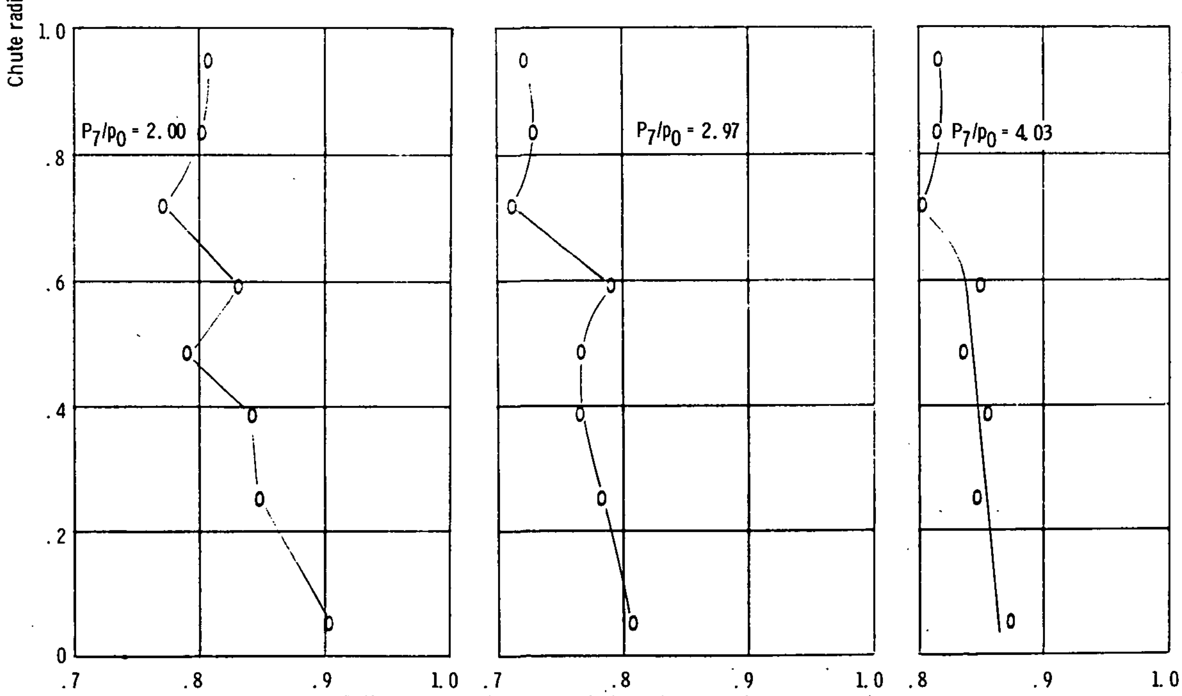

(d) With setback ejector; free-stream Mach number, M_0, 0.36.

Figure 23. - Continued.

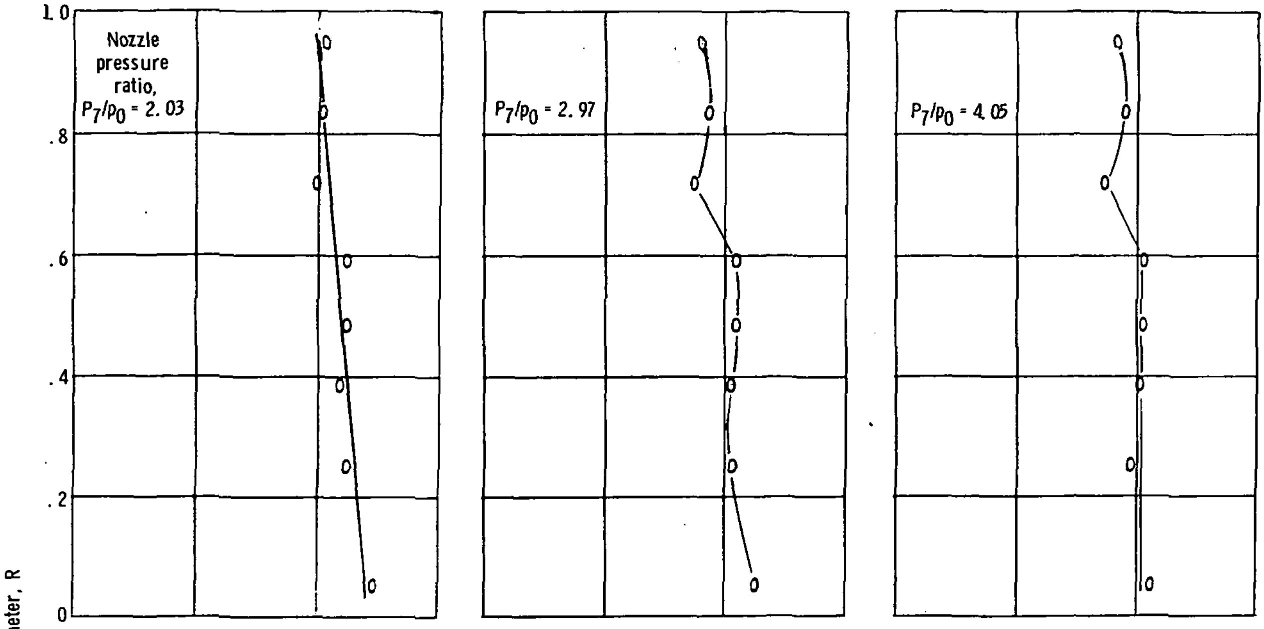

(e) With large-inlet ejector; free-stream Mach number, M_0, 0.

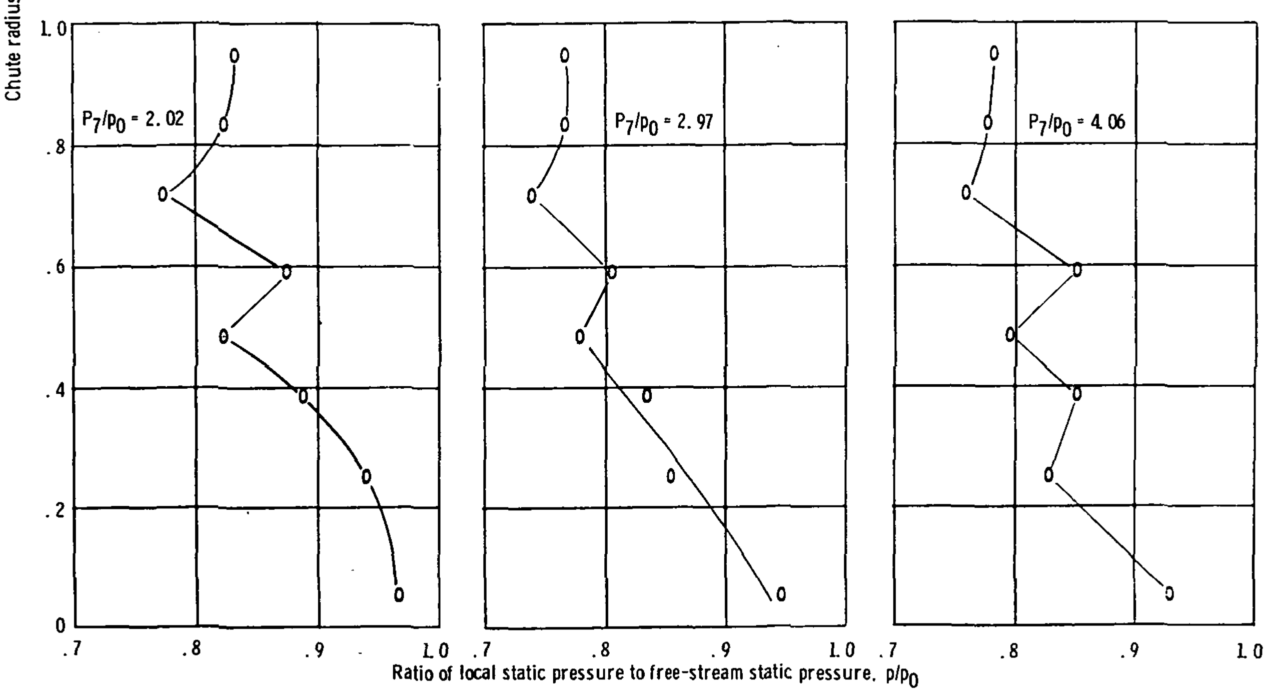

(f) With large-inlet ejector; free-stream Mach number, M_0, 0.36.

Figure 23. - Concluded.

NASA-Langley, 1975 E-8334

"The aeronautical and space activities of the United States shall be conducted so as to contribute . . . to the expansion of human knowledge of phenomena in the atmosphere and space. The Administration shall provide for the widest practicable and appropriate dissemination of information concerning its activities and the results thereof."

—NATIONAL AERONAUTICS AND SPACE ACT OF 1958

NASA SCIENTIFIC AND TECHNICAL PUBLICATIONS

TECHNICAL REPORTS: Scientific and technical information considered important, complete, and a lasting contribution to existing knowledge.

TECHNICAL NOTES: Information less broad in scope but nevertheless of importance as a contribution to existing knowledge.

TECHNICAL MEMORANDUMS: Information receiving limited distribution because of preliminary data, security classification, or other reasons. Also includes conference proceedings with either limited or unlimited distribution.

CONTRACTOR REPORTS: Scientific and technical information generated under a NASA contract or grant and considered an important contribution to existing knowledge.

TECHNICAL TRANSLATIONS: Information published in a foreign language considered to merit NASA distribution in English.

SPECIAL PUBLICATIONS: Information derived from or of value to NASA activities. Publications include final reports of major projects, monographs, data compilations, handbooks, sourcebooks, and special bibliographies.

TECHNOLOGY UTILIZATION PUBLICATIONS: Information on technology used by NASA that may be of particular interest in commercial and other non-aerospace applications. Publications include Tech Briefs, Technology Utilization Reports and Technology Surveys.

Details on the availability of these publications may be obtained from:

SCIENTIFIC AND TECHNICAL INFORMATION OFFICE

NATIONAL AERONAUTICS AND SPACE ADMINISTRATION

Washington, D.C. 20546